NASA/TM—2004–213283

NASA Marshall Space Flight Center Barrel-Shaped Asymmetrical Capacitor

J.W. Campbell, M.R. Carruth, D.L. Edwards, A. Finchum, G. Maxwell, and S. Nabors
Marshall Space Flight Center, Marshall Space Flight Center, Alabama

L. Smalley
The University of Alabama in Huntsville, Huntsville, Alabama

D. Huston, D. Ila, R. Zimmerman, C. Muntele, and I. Muntele
Alabama A&M University

June 2004

The NASA STI Program Office…in Profile

Since its founding, NASA has been dedicated to the advancement of aeronautics and space science. The NASA Scientific and Technical Information (STI) Program Office plays a key part in helping NASA maintain this important role.

The NASA STI Program Office is operated by Langley Research Center, the lead center for NASA's scientific and technical information. The NASA STI Program Office provides access to the NASA STI Database, the largest collection of aeronautical and space science STI in the world. The Program Office is also NASA's institutional mechanism for disseminating the results of its research and development activities. These results are published by NASA in the NASA STI Report Series, which includes the following report types:

- TECHNICAL PUBLICATION. Reports of completed research or a major significant phase of research that present the results of NASA programs and include extensive data or theoretical analysis. Includes compilations of significant scientific and technical data and information deemed to be of continuing reference value. NASA's counterpart of peer-reviewed formal professional papers but has less stringent limitations on manuscript length and extent of graphic presentations.

- TECHNICAL MEMORANDUM. Scientific and technical findings that are preliminary or of specialized interest, e.g., quick release reports, working papers, and bibliographies that contain minimal annotation. Does not contain extensive analysis.

- CONTRACTOR REPORT. Scientific and technical findings by NASA-sponsored contractors and grantees.

- CONFERENCE PUBLICATION. Collected papers from scientific and technical conferences, symposia, seminars, or other meetings sponsored or cosponsored by NASA.

- SPECIAL PUBLICATION. Scientific, technical, or historical information from NASA programs, projects, and mission, often concerned with subjects having substantial public interest.

- TECHNICAL TRANSLATION. English-language translations of foreign scientific and technical material pertinent to NASA's mission.

Specialized services that complement the STI Program Office's diverse offerings include creating custom thesauri, building customized databases, organizing and publishing research results…even providing videos.

For more information about the NASA STI Program Office, see the following:

- Access the NASA STI Program Home Page at ***http://www.sti.nasa.gov***

- E-mail your question via the Internet to help@sti.nasa.gov

- Fax your question to the NASA Access Help Desk at 301–621–0134

- Telephone the NASA Access Help Desk at 301–621–0390

- Write to:
  NASA Access Help Desk
  NASA Center for AeroSpace Information
  7121 Standard Drive
  Hanover, MD 21076–1320
  301–621–0390

NASA/TM—2004–213283

NASA Marshall Space Flight Center Barrel-Shaped Asymmetrical Capacitor

J.W. Campbell, M.R. Carruth, D.L. Edwards, A. Finchum, G. Maxwell, and S. Nabors
Marshall Space Flight Center, Marshall Space Flight Center, Alabama

L. Smalley
The University of Alabama in Huntsville, Huntsville, Alabama

D. Huston, D. Ila, R. Zimmerman, C. Muntele, and I. Muntele
Alabama A&M University

National Aeronautics and
Space Administration

Marshall Space Flight Center • MSFC, Alabama 35812

June 2004

Acknowledgments

The noteworthy contributions to the NASA Marshall Space Flight Center Barrel-Shaped Asymmetrical Capacitor by the following individuals and organizations that helped make this Technical Memorandum possible are greatly appreciated: James McGroary, Lisa Hughes, Vernotto McMillan, Steve Roy, Jeff Cameron; Rodney Bradford, United Applied Technologies; The University of Alabama in Huntsville; Dr. Al Sanders, the University of Tennessee; Francis Canning, Institute for Scientific Research, West Virginia; Oak Ridge National Laboratories; and Alabama A&M University.

TRADEMARKS

Available from:

NASA Center for AeroSpace Information
7121 Standard Drive
Hanover, MD 21076–1320
301–621–0390

National Technical Information Service
5285 Port Royal Road
Springfield, VA 22161
703–487–4650

TABLE OF CONTENTS

LIST OF FIGURES

LIST OF FIGURES (Continued)

LIST OF FIGURES (Continued)

LIST OF FIGURES (Continued)

LIST OF TABLES

LIST OF ACRONYMS AND ABBREVIATIONS

ETS	engineering test satellite
LeRC	Lewis Research Center
MHD	magnetohydrodynamics
mlb	millipound
MSFC	Marshall Space Flight Center
NACAP	NASA Barrel-Shaped Asymmetrical Capacitor
NSSTC	National Space Science Technology Center
SERT	space electric rocket test
STP	standard temperature and pressure
TM	Technical Memorandum
U.S.	United States
XIPS	xenon ion propulsion system

NOMENCLATURE

b	initial angular velocity at t=0
d	rotor moment arm
d_{NACAP}	NACAP diameter
I	moment of inertia
I_{arm}	moment of inertia of rotary test bed arm
I_{axle}	moment of inertia of rotary test bed axle
I_n	moment of inertia of N elements forming a complex shape
I_{NACAP}	moment of inertia of NACAP
I_{sp}	specific impulse
I_{total}	total moment of inertia of NACAP mounted in rotary test bed
k	$=1.38\times10^{-3}$ J/K
l_{arm}	length of rotary test bed arm
l_{NACAP}	length of NACAP
m	slope of curve
m_{arm}	mass of rotary test bed arm
m_{axle}	mass of rotary test bed axle
m_i	ith mass
m_{NACAP}	NACAP mass
N_A	Avogadro's number
P	pressure
$\overrightarrow{P_T}$	total momentum
R	=8.31 J/mole K
r_{arm}	radius of rotary test bed arm

NOMENCLATURE (Continued)

r_{axle}	radius of rotary test bed axle
r_{NACAP}	radius of NACAP
T	temperature
t	time
t_1	first time
t_2	second time
T_{max}	maximum thrust
T_{NACAP}	NACAP thrust
V	voltage
$\bar{v}$	molecular average speed
$\vec{v}_i$	velocity of the *i*th particle
α	angular acceleration
θ	angle
λ	mean free path
τ	torque
τ_R	total resistive torque
τ_T	torque due to thrust
ω	angular speed

TECHNICAL MEMORANDUM

NASA MARSHALL SPACE FLIGHT CENTER BARREL-SHAPED ASYMMETRICAL CAPACITOR

1. INTRODUCTION

Generating thrust in air with no moving parts and no conventional propellants, the NASA Barrel-Shaped Asymmetrical Capacitor (NACAP) offers the potential for future aerospace applications. Optimization engineering and evaluation testing are required to determine whether the technology may compete successfully with other more mature propulsion technologies. These technologies include liquid and solid rocket propulsion; various electric propulsion approaches; and turbofan, turbojet, and propeller propulsion in air.

This Technical Memorandum (TM) provides a background and context for the technology and includes a description of how the NACAP design was derived through synthesis solely from the large public domain information base. The basic physics associated with the device's performance is reviewed, followed by a summary of experimental results obtained at Marshall Space Flight Center (MSFC). In addition, recommendations for additional investigations are made, including both experimental and theoretical paths. New configurations are recommended to increase performance and extend operations into space.

2. SYNTHESIS

Drawing solely from a number of public domain information and data sources, the basic synthesis process leading to the NACAP design may be understood. These sources are the extensive public domain NASA and United States (U.S.) Air Force electric propulsion databases, the extensive public domain Thomas Townsend Brown information and databases, and the laws of physics from a number of physics textbooks studied in schools and universities across the U.S. and around the world.

In addition, commonly accepted aerospace requirements for safety, electrical robustness, structural robustness, and systems integration formed an information base of design constraints that were synthesized along with the public domain knowledge bases to derive the NACAP design (fig. 1).

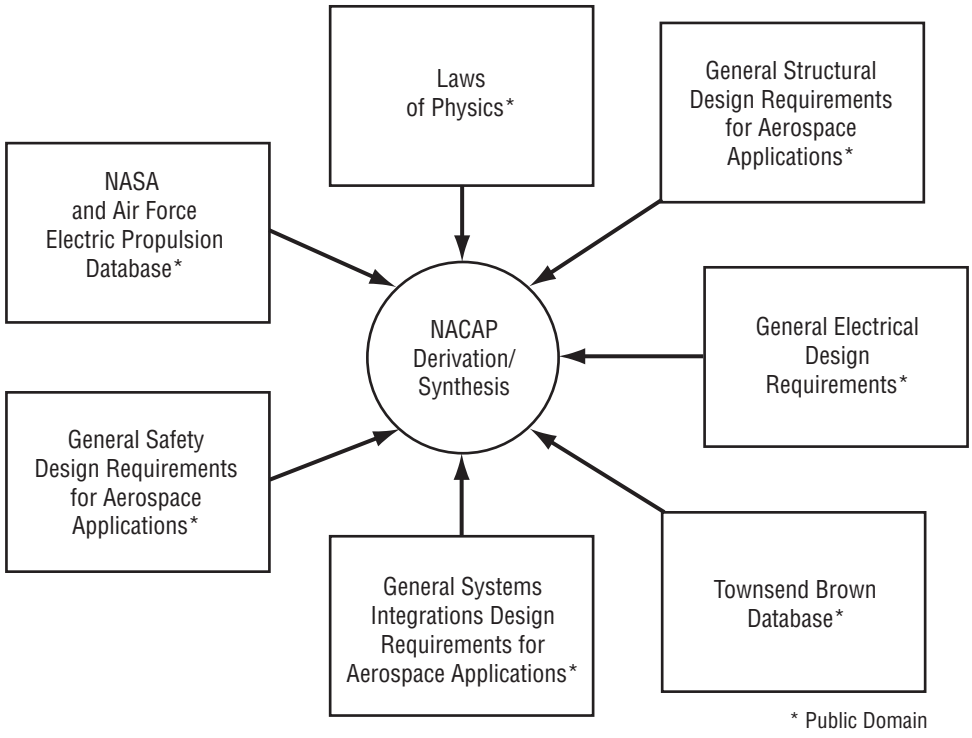

Figure 1. NACAP derivation is based solely on the tremendous volume of information and data found in the public domain.

There is a tremendous volume of information and data available in the NASA and Air Force electric propulsion information databases. The barrel-shaped configuration is common to many electric propulsion systems. All such electric thrusters operate using electric and/or magnetic fields to accelerate charged particles and, hence, achieve propulsion through action/reaction; i.e., conservation of momentum. All of these thrusters obey the basic laws of physics including Newton's laws, conservation of momentum, Maxwell's equations, and kinetic theory.

For example, Talley published a report for the U.S. Air Force in 1991 covering an extensive investigation into a specific asymmetrical capacitor design.[1] He included vacuum testing in his investigation and found that at 19 kV there was no detectable thrust in vacuum. This is one of several independent investigations that have shown no detectable thrust in vacuum from asymmetrical capacitors, as shall be described in this TM.

Other electric propulsion examples include the space electric rocket test (SERT) I at NASA Lewis Research Center (LeRC) (figs. 2–4). This 10-cm mercury ion thruster was used in a suborbital flight to successfully demonstrate ion beam neutralization in space. SERT II uses two 15-cm, 28-mN mercury ion engines from NASA LeRC to demonstrate long-term ion thruster operation in space.[2]

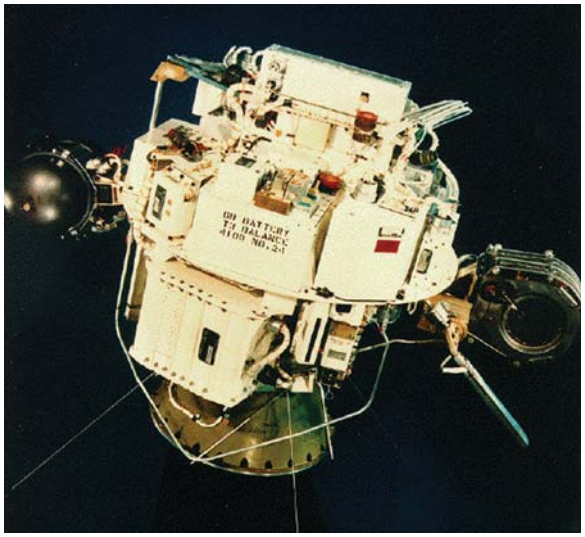

Figure 2. SERT I spacecraft.

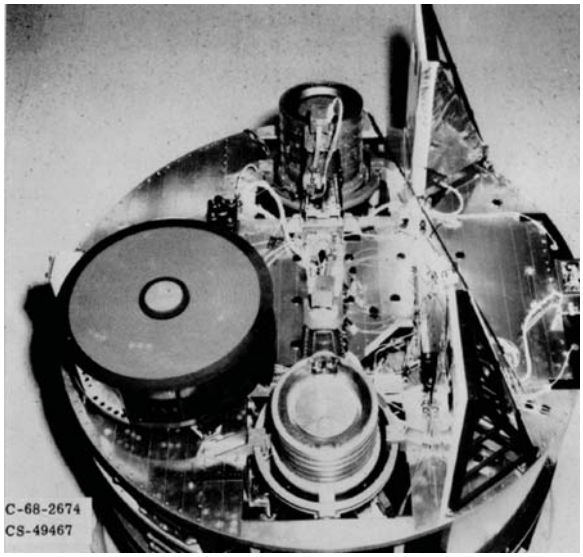

Figure 3. SERT II flight experiment.

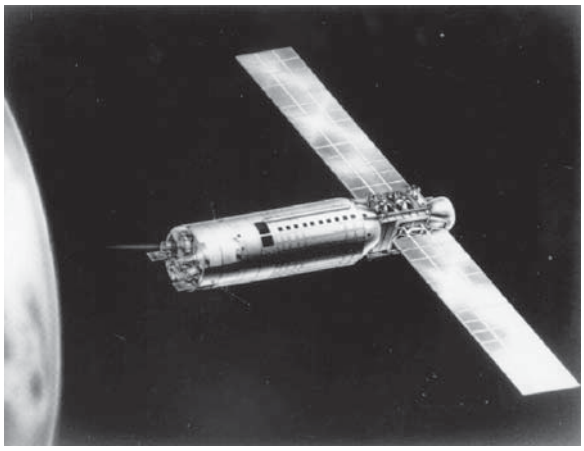

Figure 4. SERT II spacecraft.

The barrel-shaped configuration is used in a number of aerospace applications. The NASA New Millennium Program first technology demonstration spacecraft (Deep Space 1) was planned to perform an asteroid and comet flyby using the NASA Solar Electric Propulsion Technology Application Readiness (NSTAR) ion propulsion system (fig. 5). The NSTAR engine is a 30-cm diameter ion thruster using xenon as propellant. This engine requires a maximum thruster input power of 2.3 kW to provide 92 mN of thrust with a specific impulse (I_{sp}) of 3,300 lbf-s/lbm (32,340 m/s).

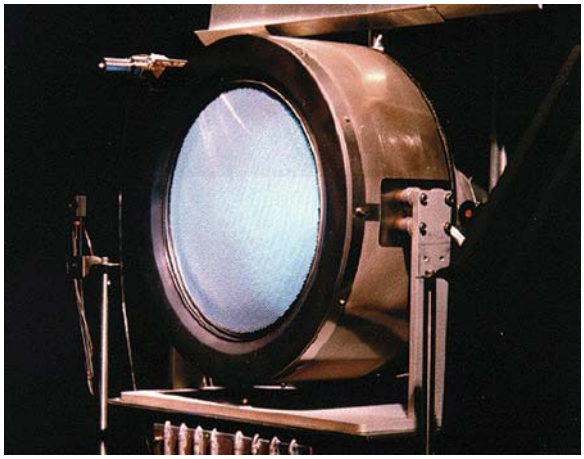

Figure 5. NSTAR thruster.

Deep Space 1 was launched from Cape Canaveral on October 24, 1998. During its primary mission, it tested several advanced, high-risk technologies in space. Later, it encountered Comet Borrelly and returned images and other science data.[2]

The UK–10 is a 10-cm diameter ion thruster that uses xenon as propellant. This thruster has a divergent-field discharge chamber design and employs electromagnets rather than the permanent magnets used in U.S. ion thrusters. At 660 W of input power, this thruster produces 25 mN of thrust with an I_{sp} of ≈3,350 lbf-s/lbm (32,800 m/s) and a thruster efficiency of ≈60 percent.[2]

AEA Technology in Culham, England, has been developing the UK–10 ion thruster (fig. 6) as well as a larger version, the UK–25, and, more recently, the ESA–XX ion thruster as part of the UK national program directed by the Space Department at the Royal Aircraft Establishment, Farnborough, England. The UK–10 may be used primarily for satellite stationkeeping or possibly attitude control. The ESA–XX ion thruster was developed in collaboration with other European companies. This 6-kW, 200-mN thruster is aimed at providing the propulsion requirements for future interplanetary space missions as well as for orbit-raising applications near Earth.[2]

Using the HS 601HP bus, Boeing Satellite Systems, based in El Segundo, CA, markets a 13-cm diameter xenon ion propulsion system (XIPS) for commercial satellites (fig. 7). The XIPS nominally requires 440 W and produces an I_{sp} of ≈2,600 lbf-s/lbm (25,480 m/s) with an efficiency of 51.3 percent. In addition, Boeing has a higher power, 25-cm diameter, 18-kW thruster for use on their HS 702 spacecraft bus that produces 3,800 seconds I_{sp} and 165 mN of thrust.[2]

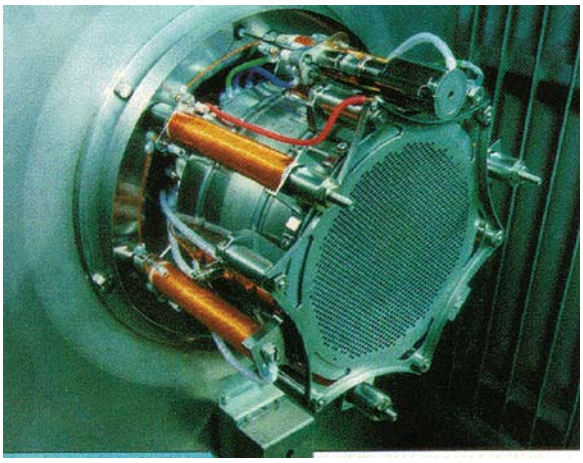

Figure 6. UK–10 ion thruster.

Figure 7. XIPS at Boeing Satellite Systems.

The ion propulsion system shown in figure 8 was developed to provide north-south station-keeping for the Engineering Test Satellite VI (ETS–VI). Two 12-cm-diameter, divergent-field xenon ion engines are shown. The spacecraft was launched in 1995 but never achieved operational orbit due to a failure of the launch vehicle upper stage. The spacecraft was stranded in a highly elliptical orbit passing through Earth's radiation belts. All four ion engines were successfully tested before extensive radiation damage to the solar arrays prevented further operation of the ion propulsion system.[2]

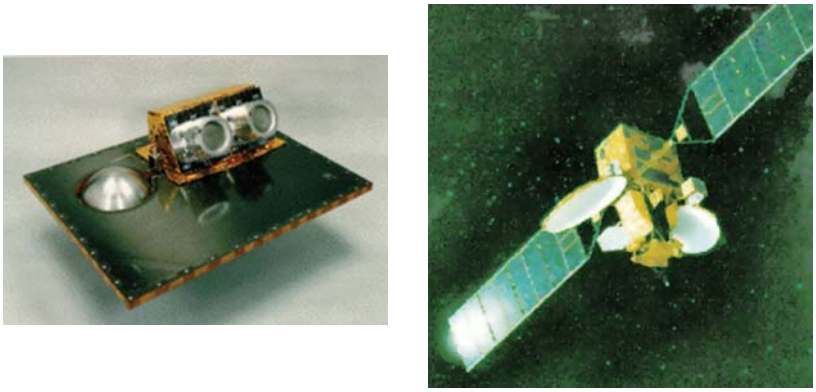

Figure 8. Japanese ETS–VI ion propulsion system.

Figure 9 shows a demonstration of a 10-kW ion propulsion module assembled in 1987 at the Jet Propulsion Laboratory in Pasadena, CA, for Mariner Mark II applications. Two modified J-series 30-cm diameter ion engines are shown on the module. Each engine is capable of operating at 5 kW with a thrust on the order of 0.2 N and an I_{sp} of 3,800 lbf-s/lbm with xenon propellant. The NACAP in air promises much better thrust per power performance.[2]

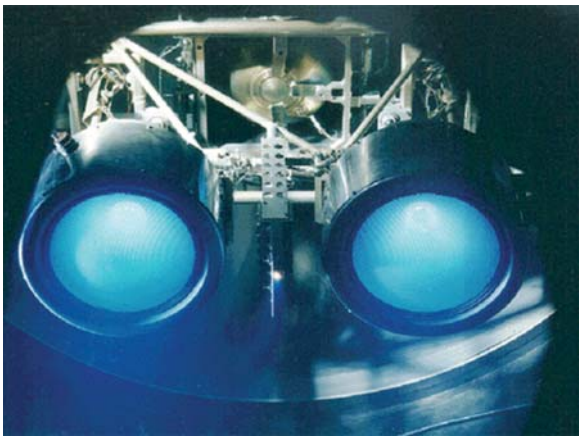

Figure 9. Modified J-series thruster.

These examples indicate that another important part of the thruster or design synthesis process is to factor in general aerospace requirements. For example, extended surfaces at high potential are dangerous to ground crews and associated vehicle electronics and may severely constrain application. Transportation vehicle charging is another concern both in space and air. Static discharges can wreak havoc with onboard electronics, computers, and avionics. A barrel-shaped configuration should enable convenient containment strategies such as thruster isolation on the tip of a wing or boom.

Aerospace applications require light, yet structurally robust designs to withstand aerodynamic loads in the atmosphere and/or launch and reentry loads. Fatigue considerations are also important both in air and space. Thrust must be transferred from the propulsion system to the vehicle through a robust structural interface. As with many other aerospace propulsion systems, a barrel-shaped configuration enables a structurally robust design to meet these criteria.

Performance is highly dependent upon the electrical fidelity of the design. Working at high voltages is difficult due to potential surface conduction on dielectric materials leading to electrical breakdowns. A barrel-shaped configuration should be more electrically compatible with aerospace applications and should eliminate any cathode edge effect losses.

Propulsion component design for aerospace applications must be integrated into a total system. A barrel-shaped configuration follows the strategy seen for a diverse group of prior and existing propulsion systems including turbine and turboprop airbreathing engines as well as solid, liquid, and electric rocket engines. Hence, a barrel-shaped configuration enables optimum systems integration while at the same time enabling sound safety and structural engineering requirements to be achieved.

Another important aspect of this synthesis is derived from the laws of physics as taught in numerous texts across the U.S. Although the NACAP is relatively basic in design, in operation the interactions between materials, particles, and fields are complex. The behavior of the NACAP can be fully explained by the careful application of the laws of physics. This includes mechanics, dynamics, Newton's three laws of motion, the law of conservation of momentum, electricity and magnetism, Coulomb's law, Maxwell's equations, thermodynamics, kinetic theory, relativity, and quantum mechanics. These areas, when appropriately combined in a fluid context, constitute the field of magnetohydrodynamics (MHD). The NACAP is an MHD device.

Townsend Brown's extensive public domain information and databases are also part of this synthesis (table 1). For example, some of his earliest work is reflected in his 1928 British patent detailed in reference 3 (fig. 10). In this patent he teaches both flat plate and general cylindrical configurations.

Another example is one of Townsend Brown's U.S. patents published in 1960 (fig. 11).[4] In this patent he teaches that ion acceleration and the subsequent action-reaction are the basic physical mechanisms producing thrust. He also teaches using a rotational platform as well as a basic flat asymmetrical capacitor; the basic flat asymmetrical capacitor is the building block from which more advanced designs may be synthesized. Asymmetry in this context refers to the geometrical asymmetry between oppositely charged conductive elements of the capacitor. The basic flat plate capacitor as seen in sophomore physics texts would be a counterexample of a symmetrical capacitor. Townsend Brown also teaches that making the smaller conductive element positive provides greater thrust performance.

Table 1. Sampling of Townsend Brown's patents illustrating the tremendous amount of information available in the public domain.

Country	Patent Number	Title	Date Issued
Australia	49,960	Beneficiation of Gravitational Isotopes	
Canada	675,966	Electrohydrodynamic Fluid Pump	12/10/63
	726,958	Method for Beneficiation of and Devices Employing Gravitational Isotopes	2/1/66
	771,815	Electrohydrodynamic Sound Devices	11/14/67
	876,356	Fluid Control System	7/20/71
France	1,207,519	Electrokinetic Methods	9/15/59
	1,246,669	Electrohydrodynamic Pump	
Germany	W25839IVc/12E	Beneficiation of Gravitational Isotopes	
Great Britain	300,311	Method of Producing Force or Motion	11/15/28
	20415/59	Beneficiation of Gravitational Isotopes	
Holland	240,401	Beneficiation of Gravitational Isotopes	
Italy	33/110	Beneficiation of Gravitational Isotopes	
Japan	14819/34	Electrokinetic Methods	
	36–1066	Electrokinetic Methods	6/6/61
	19917/34	Beneficiation of Gravitational Isotopes	
Switzerland	427,509	Electrohydrodynamic Pump	
United States	1,974,483	Electrostatic Motor	9/25/34
	2,207,576	Method and Apparatus for Removing Suspended Matter from Gases	3/11/47
	2,417,347	Vibration Damper	3/11/47
	2,949,550	Electrokinetic Apparatus	8/16/60
	3,018,394	Electrokinetic Transducer	1/23/62
	3,022,430	Electrokinetic Generator	2/20/62
	3,187,206	Electrokinetic Apparatus	6/1/65
	3,196,296	Electric Generator	7/20/65
	3,267,860	Electrohydrodynamic Fluid Pump	8/23/66
	3,296,491	Method and Apparatus for Producing Ions and Electrically-Charged Aerosols	1/3/67
	3,518,462	Fluid Flow Control System	6/30/70
Other Inventors	2,588,427	Condenser Charge Regulation	

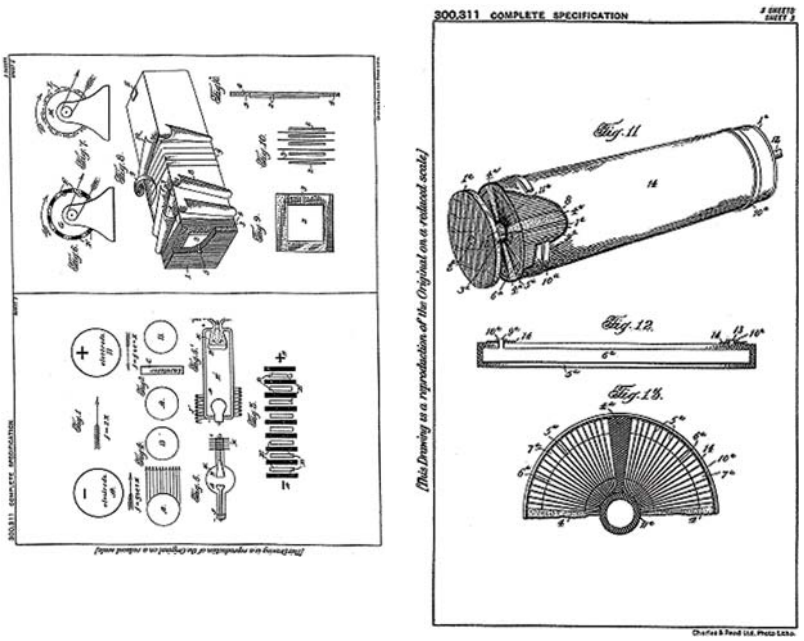

Figure 10. Drawings from Townsend Brown's 1928 public domain British patent illustrating a multiplate idea and a general cylindrical configuration.

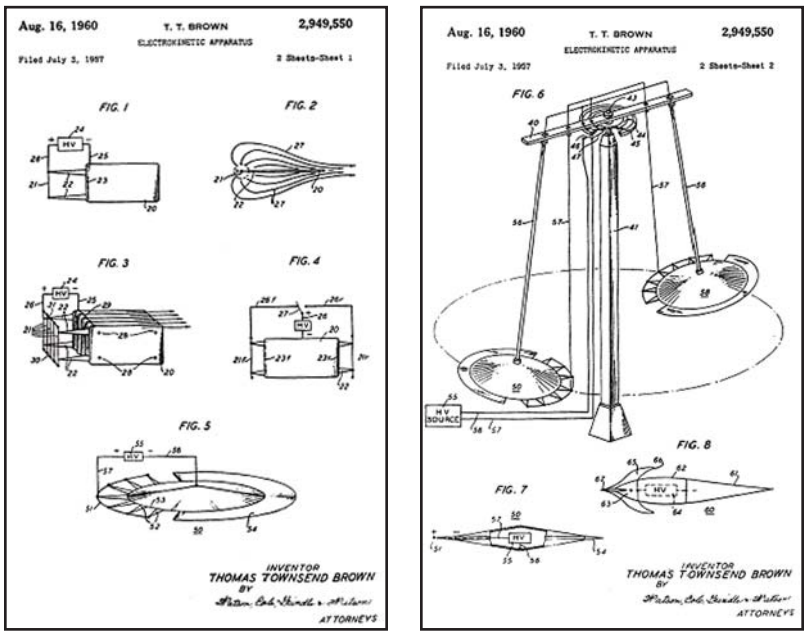

Figure 11. Drawings from Townsend Brown's 1960 public domain patent, illustrating a basic flat asymmetrical capacitor and rotary platform concept.

3. DESIGN DERIVATION

Figure 12 illustrates the building block approach for Jeff Cameron's lifter innovation. Three Townsend Brown basic flat asymmetrical capacitors are connected into a triangular cross section. Any number of triangles may then be connected to form larger triangles giving the lifter design. The triangular cross section tends to provide stability when lifting vertically. Note that the smaller conductive element is usually made the anode.

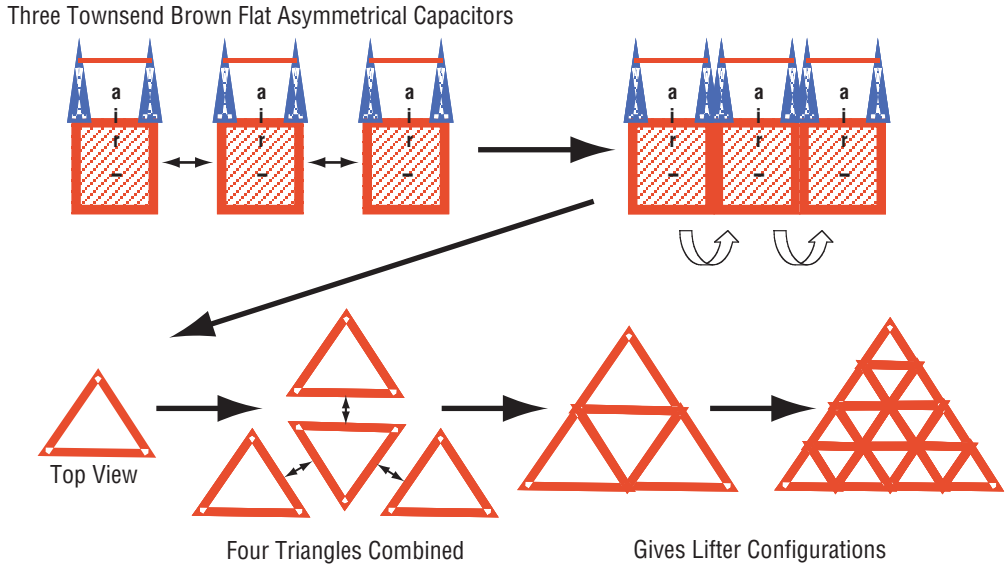

Figure 12. Derivation of the lifter from Townsend Brown's basic flat asymmetrical capacitor.

Again starting with Townsend Brown's basic flat asymmetrical capacitor and rolling it into a barrel shape provides the fundamental NACAP design innovation (fig. 13). The basic NACAP then forms the building block for a number of NACAP design innovations. Again, note that the smaller conductive element is preferred for the anode. Of course, a number of experiments have been run reversing the polarity of the capacitor. When the smaller conductive element is negative, reduced performance is typically observed. Alternating, pulsed, and variable power remain to be investigated. Certainly, some improvement in performance may be realized if a resonant pulse pattern could be found that appropriately utilizes the electrodynamics and MHD characteristics of the thrust generation process.

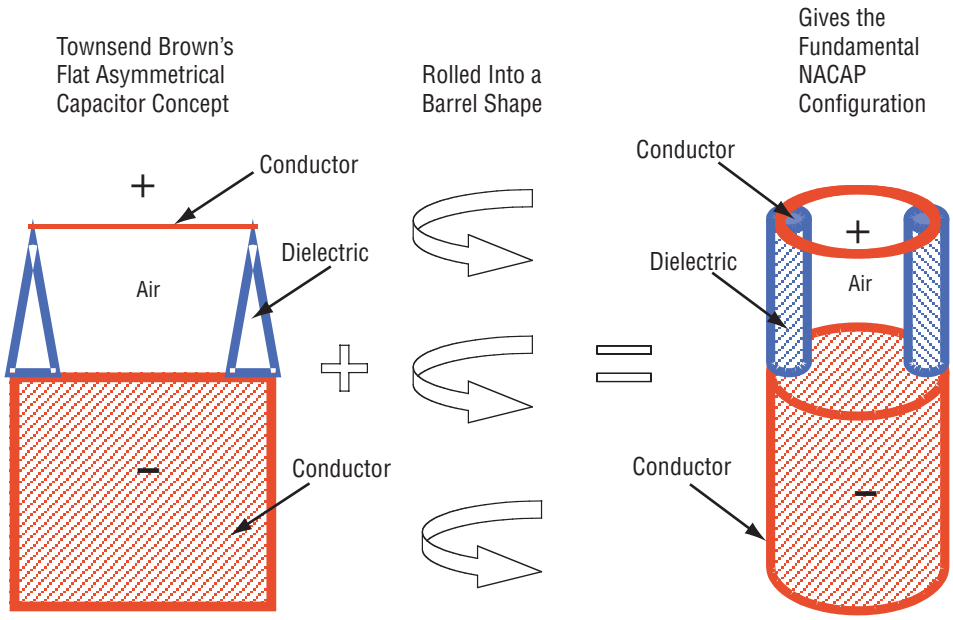

Figure 13. Rolling the Townsend Brown flat asymmetrical capacitor into a barrel shape provides the basic NACAP innovative configuration.

The NACAP-extended derivations may focus on different variables depending on the application. Maximum robustness for the aerospace environment may be the requirement or less robustness and greater sparking resistance. Figure 14 illustrates some of these evolutionary options. Clearly, for a given application, an optimization process is required to balance requirements appropriately. This is the primary thrust of MSFC NACAP research for a number of different applications. Experimental model Alpha is the primary test hardware used in this TM. Experimental model Beta that will be shown later and experimental model Gamma are follow-on devices providing greater performance due to innovative design enhancements.

Since corona formation is one source of ions for the NACAP, optimizing anode design is an area of continuing investigation (fig. 15). Again, depending upon the application, one configuration may be preferable to another. The coronal production "ears" on experimental model Alpha are an innovation courtesy of Jeff Cameron.

NASA has received two patents related to NACAP design innovations, US 6,317,310 B1[5] and US 6,411,493 B2[6] (figs. 16a–16c), and has a third patent pending that teaches additional design modifications to enable operations in space.

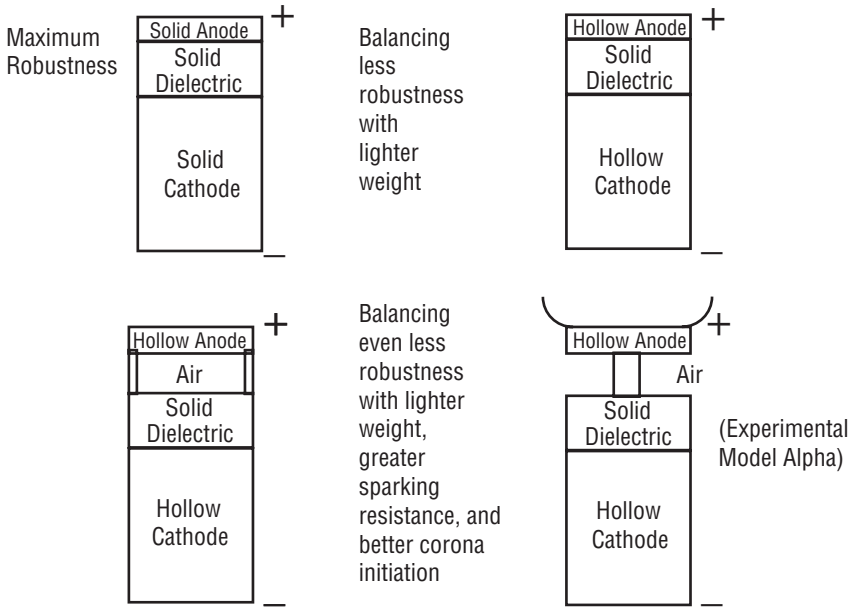

Figure 14. NACAP derivation/synthesis engineering design options evolution.

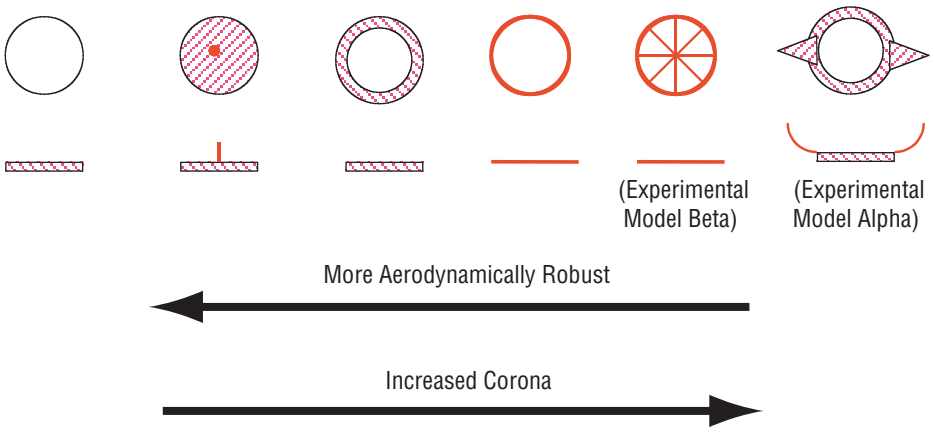

Figure 15. Anode design examples.

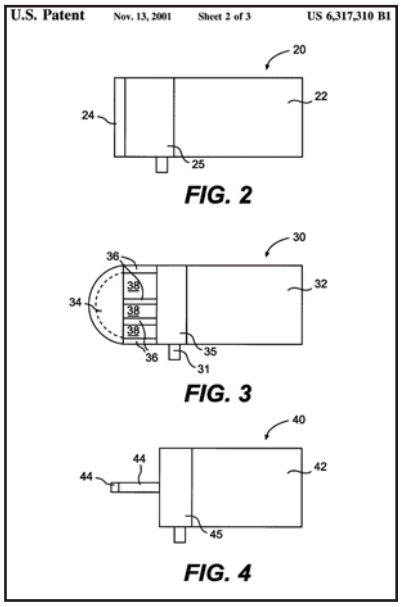

Figure 16a. Examples of various NACAP designs.

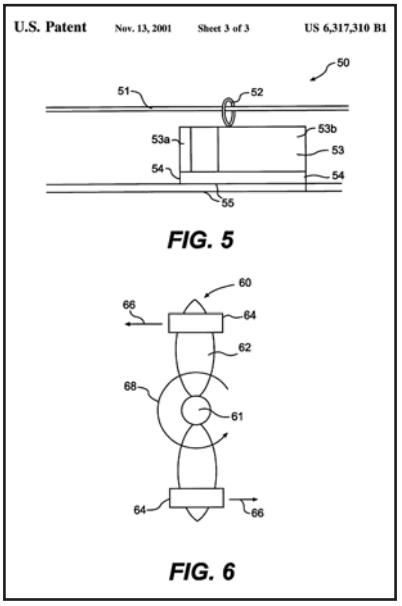

Figure 16b. Examples of potential NACAP applications.

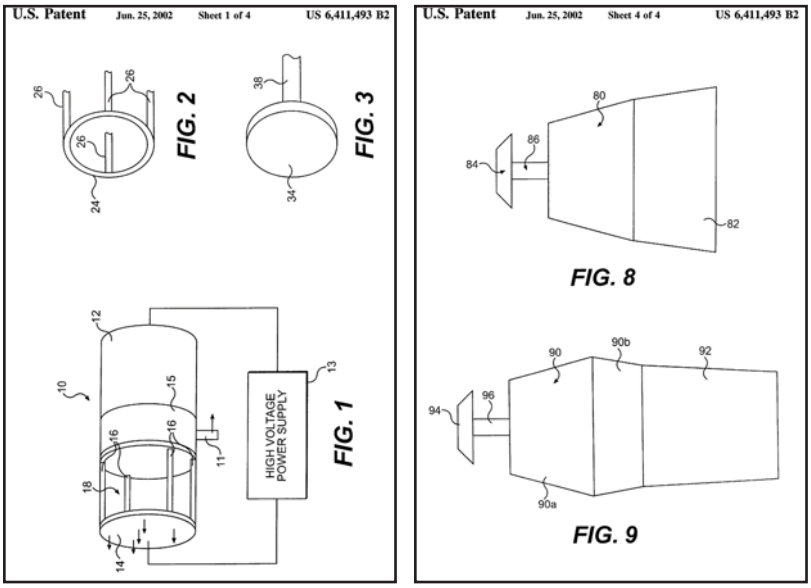

Figure 16c. Other asymmetrical capacitor design examples.

4. BASIC PHYSICS

Superficially, the NACAP appears to be an electrostatic device. Coulomb's law comes to mind immediately. Figure 17 illustrates that the force between two charged objects is dependent upon their separation as well as their charge. This basic theoretical description has been proven experimentally many times.

Looking at an example of Coulomb's law helps illustrate the promise of the NACAP due to the substantive forces available from electrostatic charge interactions. In the example provided in figure 18, the charges going through a typical 110-W household lightbulb in 1 s are collected and placed 1 m from a collection of equal charge from another lightbulb. The electrostatic repulsive force predicted by Coulomb's law is 1 million tons. Although the current through the NACAP is much less than that through a lightbulb, the separation is also much smaller than 1 m; hence, as described later in this TM, the NACAP Coulomb forces may be substantial.

Although electrostatics plays a dominant role initially in the complex operation of the NACAP, the emergence of a current implies moving charges which implies the existence of magnetic fields. One future NACAP research area is the investigation and optimization of the magnetic field contribution to the performance of the NACAP. Thus, one starts with Maxwell's equations to begin a theoretical description of the NACAP operation. Maxwell's equations may be expressed either in integral form or in differential form as shown in figure 19. Applying Maxwell's equations to describe NACAP physics is an area of theoretical investigation for the future.

Since the NACAP produces thrust, Newton's three laws of motion also should be included in a theoretical treatment. Newton's first law states that an object remains at rest or in uniform motion in a straight line unless acted upon by an external force. It may be seen as a statement about inertia, that objects remain in their state of motion unless a force acts to change the motion. Any change in motion involves an acceleration, and then Newton's second law applies.

Newton's second law, $F_{NET} = ma$, applies to a wide range of physical phenomena; however, it has limitations. It applies only where the force is the net external force. It does not apply directly when the mass is changing, either from loss or gain of material, such as a rocket. Nor does it apply if the object is traveling close to the speed of light where relativistic effects become siginificant. Nor does it apply directly to the scale of the atom where quantum mechanics effects become significant.

Newton's third law states that all forces in the universe are present in equal but oppositely directed pairs. There are no isolated individual forces. For every single external force that acts on an object there is another force of equal magnitude that acts back on the source that exerted that external force. For internal forces, a force on one part of a system will be countered by a reaction force on another part of the system. An isolated system cannot by any means exert a net force on the system as a whole. A system cannot self-start itself into motion with purely internal forces to achieve a net force and an acceleration; it has to interact with an object external to itself.

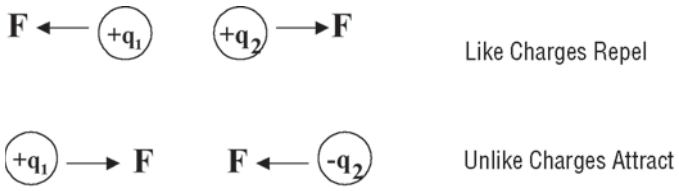

$$F = \frac{1}{4\pi\varepsilon_0}\left(\frac{q_1 q_2}{r^2}\right) = k\frac{q_1 q_2}{r^2}$$

$$k \approx 9\times10^9\ N\,m^2/C^2$$

Figure 17. Coulomb's law is applicable to the NACAP.

Power=Voltage × Current
Ampere = Coulomb/second

$$P = VI = V\frac{q}{t} \quad \Rightarrow \quad q = \frac{Pt}{V} = \frac{(110\,w)(1\,s)}{(110\,v)} = 1\ C$$

$$F = \frac{kq_1q_2}{r^2} = \frac{(9\times10^9\ N\,m^2/C^2)(1C)(1C)}{(1m)^2} = 9\times10^9\ N$$

$$1N = .225\,lb \ \Rightarrow \ F \approx 2\times10^9\ lb = 1\ million\ tons$$

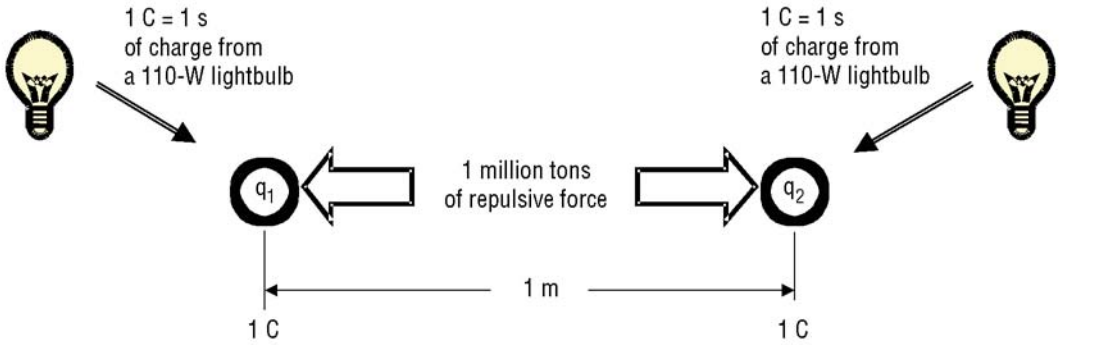

Figure 18. Example of Coulomb's law.

Gauss' Law For Electricity	$\oint \vec{E} \cdot d\vec{A} = \frac{q}{\varepsilon_0}$
Gauss' Law For Magnetism	$\oint \vec{B} \cdot d\vec{A} = 0$
Faraday's Law Of Induction	$\oint \vec{E} \cdot d\vec{s} = -\frac{d\Phi_B}{dt}$
Ampere's Law	$\oint \vec{B} \cdot d\vec{s} = \mu_0 i + \frac{1}{c^2}\frac{\partial}{\partial t}\int \vec{E} \cdot d\vec{A}$

Gauss' Law For Electricity	$\nabla \cdot E = \frac{\rho}{\varepsilon_0}$
Gauss' Law For Magnetism	$\nabla \cdot B = 0$
Faraday's Law Of Induction	$\nabla \times \vec{E} = -\frac{\partial \vec{B}}{\partial t}$
Ampere's Law	$\nabla \times \vec{B} = \frac{\vec{J}}{\varepsilon_0 C^2} + \frac{1}{C^2}\frac{\partial \vec{E}}{\partial t}$

Figure 19. Maxwell's equations are applicable to NACAP operation.

Closely related to Newton's laws is the law of conservation of momentum. The total momentum of an isolated system is a constant. The vector sum of the individual momentums of an isolated system cannot be changed by interactions inside the system. Thus only certain types of motions can occur in an isolated system. If one element of a system is given a momentum in a given direction, then some other element or elements of the system must also simultaneously be given exactly that same momentum in the opposite direction. Conservation of momentum is an absolute symmetry of nature. Nothing in nature is known that violates this fundamental law.

Defining the total momentum,

$$\overrightarrow{P_T} = \sum_1^n m_i \vec{v}_i \ , \tag{1}$$

the conservation of momentum then gives

$$\overrightarrow{P_T}(t_1) = \overrightarrow{P_T}(t_2) \ ; \tag{2}$$

Hence,

$$\sum_1^n m_i \vec{v}_i(t_1) = \sum_1^n m_i \vec{v}_i(t_2) \ . \tag{3}$$

A rocket is an excellent example of how the law of conservation of momentum may be used. Using this law the rocket equation that predicts the speed of the rocket at any particular time in its flight as a function of its mass may be derived. Based on equations shown in figure 20, if one measures experimentally all of the parameters associated with the operation of a given rocket, one will find those results to be in complete agreement with this theoretical development based on conservation of momentum. This theoretical description has been confirmed many times by experiment.

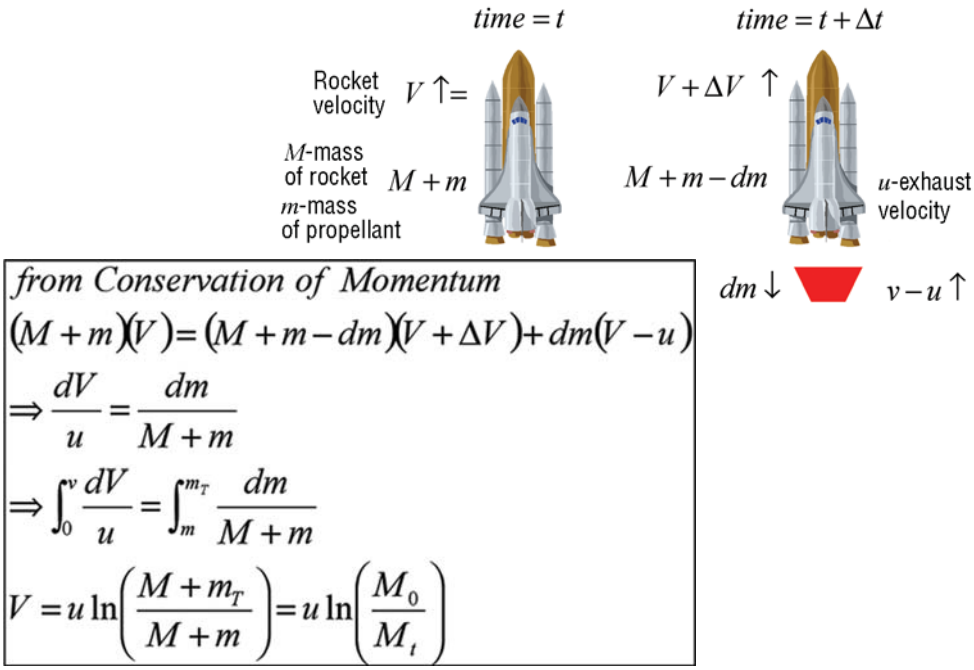

Figure 20. Rocket example of conservation of momentum.

Next, by using relationships from kinetic theory, one realizes that the number of potential charge carriers in the region near the capacitor is tremendous, offering the promise of a reservoir of tremendous force from which to draw.

Figure 21 illustrates typical dimensions associated with kinetic theory for an ideal gas. Individual molecules are exaggerated in size. A typical molecular diameter is 0.3 nm, an average molecular separation is 3.3 nm, and an average molecular separation is about 10 times the molecular diameter. The mean free path is 93 nm. Thus, for an ideal gas at standard pressure and temperature (STP) where the pressure is 760 mmHg and the temperature is 0 °C, the mean free path is 310 times the typical atomic diameter and 28 times the average molecular separation. The collision frequency is on the order of 10^{10} collisions/s.

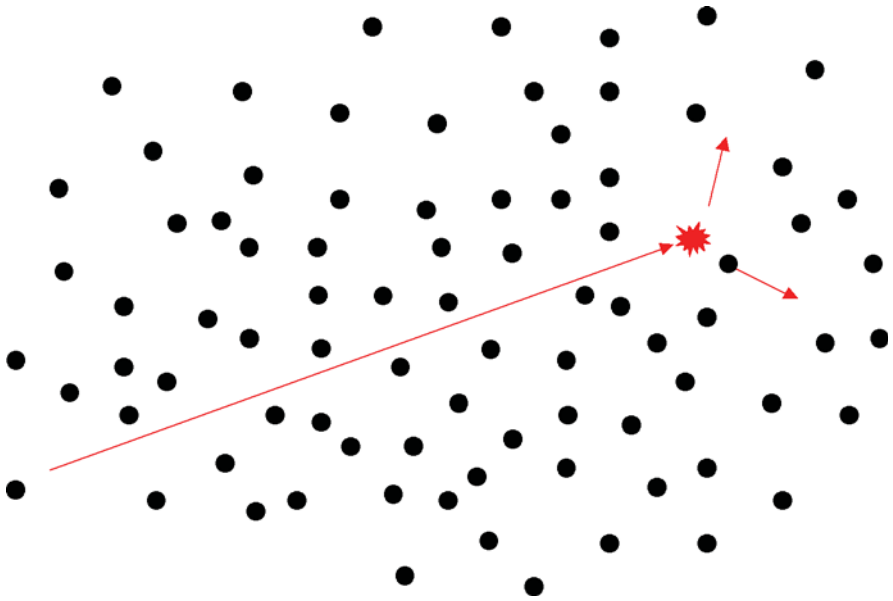

Figure 21. Illustration of mean free path.

The ideal gas law is represented by $PV = nRT$, where $R = 8.31$ J/mole K. The molecular average speed is

$$\bar{v} = \sqrt{\frac{8kT}{\pi m}} \ , \tag{4}$$

where $k = 1.38\times10^{-23}$ J/K. The molecular mean free path is

$$\lambda = \frac{RT}{\sqrt{2}\pi d^2 N_A P} \ , \tag{5}$$

where $N_A = 6.02\times10^{23}$ and $d \approx 0.3\times10^{-9} m$.

Magnetic and electric fields influence many natural and manmade fluids. They are used to heat, pump, stir, and lift. Examples include Earth's magnetic field that is maintained by fluid motion in Earth's core, the solar magnetic field that generates sunspots and solar flares, and the galactic field that influences the formation of stars. Dynamics, electrodynamics, electrohydrodynamics, and MHD include the study of the interaction of magnetic and electric fields, conducting and nonconducting bodies, and fluids. Clearly, the relatively basic NACAP configurations give rise to extraordinarily complex interactions between plasmas; charged and neutral bodies; charged particles and currents; and neutral particles and flows that may be comprehensively described by an MHD formulation:

$$\frac{\partial \rho}{\partial t} + \nabla \bullet \left(\rho \vec{u}\right) = 0$$

$$\partial \frac{d\vec{u}}{dt} = \vec{j} \times \vec{B} - \nabla p$$

$$\vec{j} = \sigma\left(\vec{E} + \vec{u} \times \vec{B}\right)$$

$$\nabla \times \vec{B} = \mu_0 \vec{j} + \mu_0 \varepsilon_0 \frac{\partial \vec{E}}{\partial t}$$

$$\nabla \times \vec{E} = \frac{\partial \vec{B}}{\partial t}$$

$$\nabla \bullet \vec{B} = 0$$

$$\nabla \bullet \vec{u} = 0 \ . \qquad (6)$$

5. EXPERIMENTAL RESULTS

Three experimental hardware configurations were developed at the National Space Science and Technology Center (NSSTC), NASA MSFC, and The University of Alabama in Huntsville. Most experimental results were initially obtained using NACAP model Alpha. Models Beta and Gamma served to confirm the results obtained in Alpha and verified that optimization could provide higher performance. The Institute for Scientific Research located in Fairmont, WV, independently investigated the NACAP and verified our findings (F. Canning, Institute for Scientific Research, Private Communication, 2003–2004).

In figure 22, the region immediately surrounding the NACAP is a complex, extraordinarily dynamic combination of intense electric fields; magnetic fields; carbon dioxide, water vapor, oxygen, nitrogen and other trace gases in ion, atomic, and/or molecular states; ablation products; and plasma (corona) interacting through multiple physical laws.

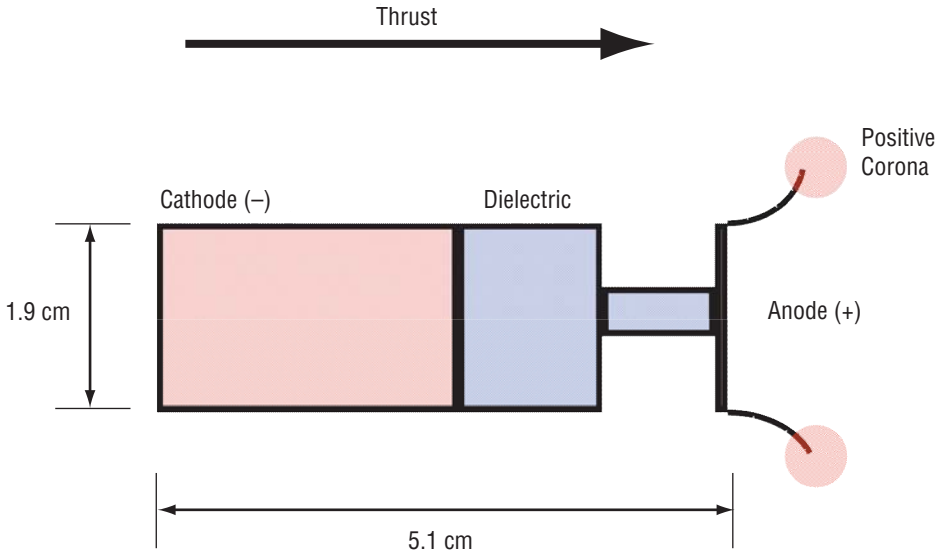

Figure 22. Experimental hardware configuration—NACAP model Alpha.

In his 1960 public domain patent, Townsend Brown teaches a rotational platform application. A rotary test bed (fig. 23) was also selected for NACAP testing as it provides positive proof of thrust generation, allows for an accurate measurement of the thrust, and enables testing in low-cost vacuum chambers. There is no plan nor has there ever been an attempt by the authors to patent a rotational test bed.

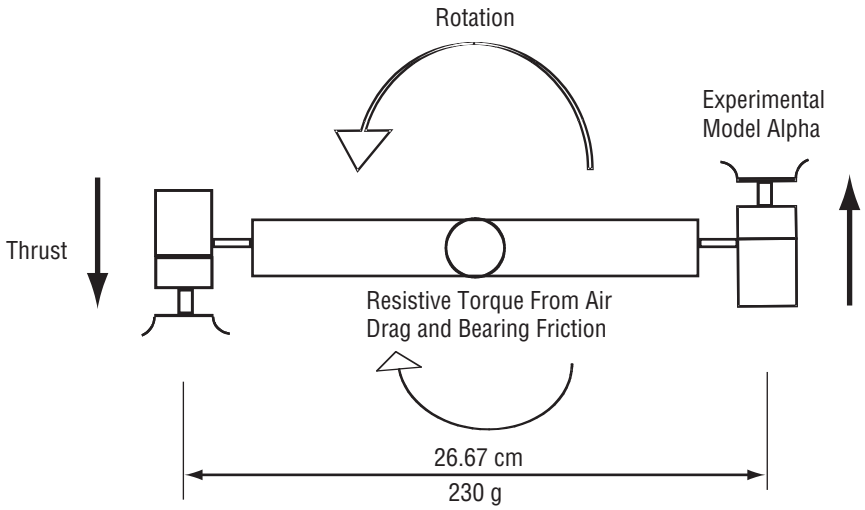

Figure 23. NACAP experimental hardware rotary test bed.

Utilizing a rotary test bed enables the accurate calculation of the thrust by determining the moment of inertia, measuring the angular velocity of the rotation, and by measuring the resistive torque. The torque is a combination of air resistance and bearing friction. The moment of inertia may be determined two independent ways. First, it can be calculated from the geometry and masses of the test bed rotor and the two mounted NACAPs. The following equations show this approach:

$$I_{\text{total}} = \sum I_n = I_{\text{axle}} + I_{\text{arm}} + I_{\text{NACAP}} \quad . \tag{7}$$

Using the parallel axis theorem,

$$I_{\text{total}} \approx m_{\text{axle}} r_{\text{axle}}^2 + \frac{1}{2} m_{\text{arm}} r_{\text{arm}}^2 + \frac{1}{12} m_{\text{arm}} l_{\text{arm}}^2 + \frac{1}{2} m_{\text{NACAP}} r_{\text{NACAP}}^2 + \frac{1}{12} m_{\text{NACAP}} l_{\text{NACAP}}^2 + m_{\text{NACAP}} d_{\text{NACAP}}^2 \quad . \tag{8}$$

Second, the rotor may be suspended from a torsional pendulum. If the pendulum has already been calibrated, the moment of inertia should be easily calculated from the harmonic motion of the pendulum. Calibrating the pendulum using a known test mass is relatively straightforward as well.

A cylindrical weight may be used to calibrate the suspension fiber. A piano wire would be a good choice. The moment of inertia of the weight is easily calculated from its mass and geometry. By observing its torsional harmonic motion suspended from the wire, one may calculate the spring constant for the wire. Once the spring constant is known, the moment of inertia of the rotor assembly may easily be determined.

Figure 24 shows two NACAPs mounted in an experimental rotary platform in preparation for vacuum testing. Typical operating parameters are 27,000 V providing a steady state rotation of 60 RPM and drawing 20 μA of current at STP.

Returning to Coulomb's law example (fig. 25), NACAP peak thrust has been observed to be a few millipounds at a peak current of 20 μA. If the analysis is performed using the observed parameters from experimentation, the Coulomb forces for one second's accumulative charge may be found to be substantive. Clearly significant promise for greater performance is indicated.

- Number of molecules$_{\text{near vicinity}} = 9.04\times10^{21}$
- Equivalent Coulomb force$_{20\times10^{-6}\ \text{A}} = 2{,}000$ lb
- Equivalent Coulomb force$_{2\ \text{NACAPs}} = 4{,}000$ lb

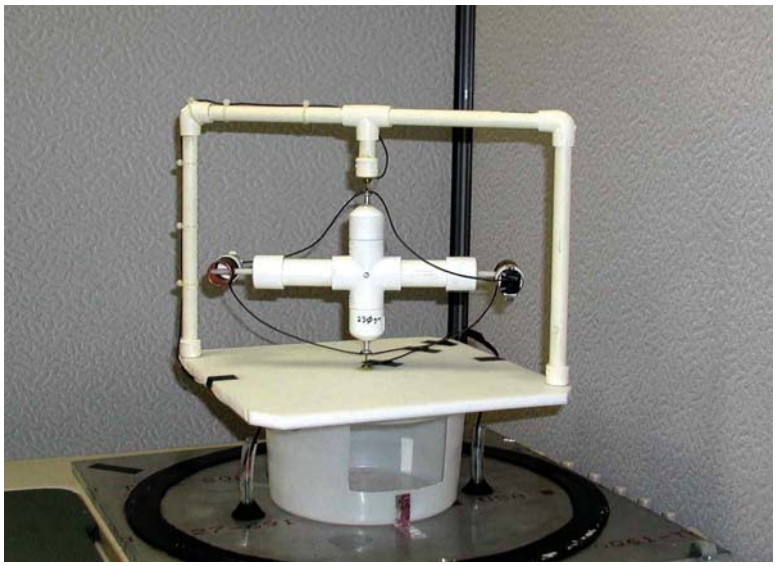

Figure 24. NACAP experimental model Alpha mounted in rotary test bed.

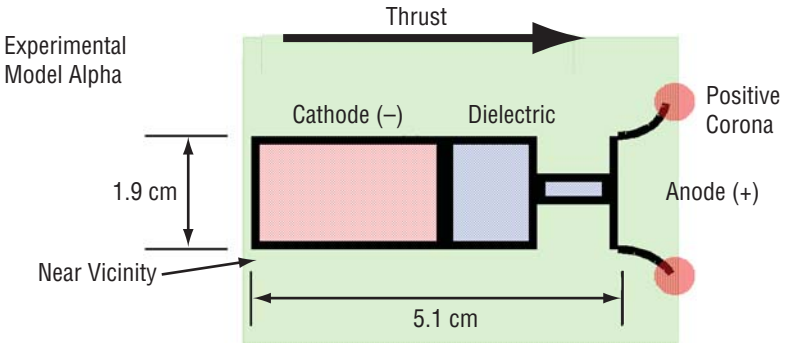

Figure 25. The near NACAP vicinity.

Spin-down measurements indicate that the combined resistance due to drag and bearing friction is essentially linear. Figure 26 shows example measurements taken from several experimental runs. Angular velocity as a function of time is plotted. The rotor assembly with the NACAP at zero potential is spun upward to 60–70 RPM. The rotor is then allowed to free spin while its angular deceleration due to air resistance and bearing resistance is measured. The spin down may be approximated accurately by a linear curve. This implies that the primary contribution to resistance to rotation is bearing friction while air resistance at these speeds is only secondary.

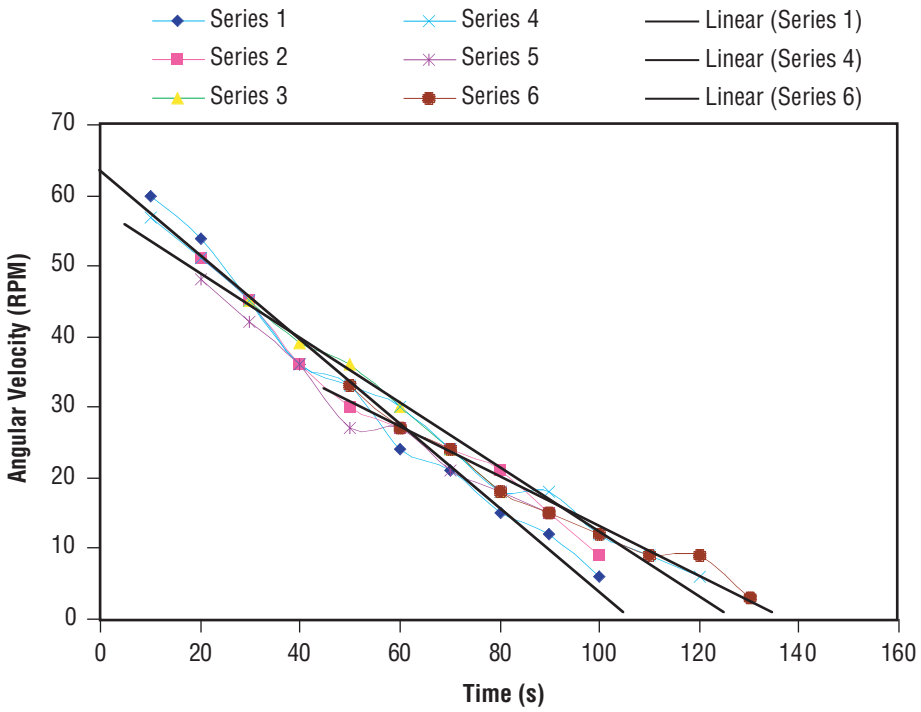

Figure 26. NACAP spin-down data.

Figure 27 illustrates a typical experimental dataset showing NACAP rotor RPM as a function of voltage across the NACAP. As voltage is increased from zero, no rotation is observed until the thrust exceeds the static friction bearing resistance. At this point, rotation initiates. Thrust initiates earlier but is not measurable by this experimental approach until rotation begins. As the voltage increases so does the thrust. At ≈28 kV for this particular NACAP configuration with extensive operating experience under laboratory conditions, 60 RPM is achieved at steady state. If the voltage is increased above this ceiling, random sparking events initiate. The experiment is terminated at this point to avoid damage to the NACAP. Clearly, a design objective would be to raise the sparking threshold and increase thrust at the same time.

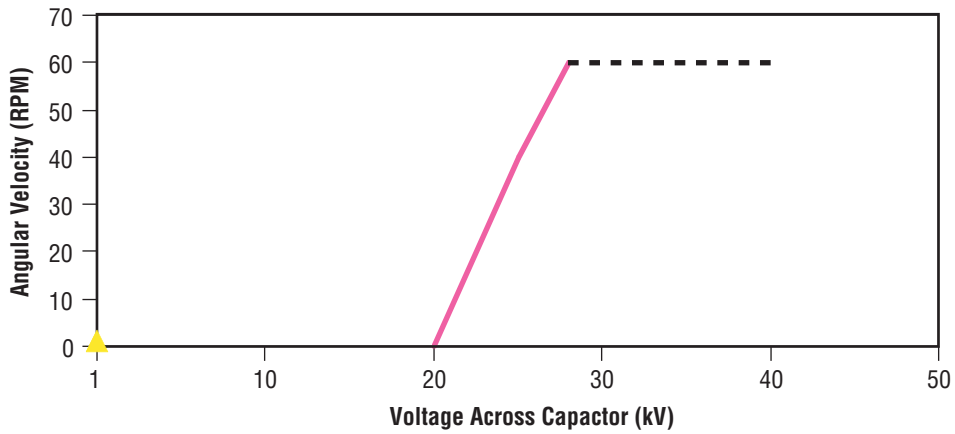

Figure 27. NACAP RPM versus voltage showing upper and lower operating boundaries.

Figure 28 shows the average current as a function of voltage for a typical NACAP experimental run. While the instantaneous currents fluctuate dramatically, the average current is well behaved as is evidenced by the smooth steady state motion of the rotor at optimum operating conditions. The wild fluctuations in the instantaneous current indicate the complex MHD mechanisms at work on extremely short timescales. An analysis of the instantaneous current is an area for future work.

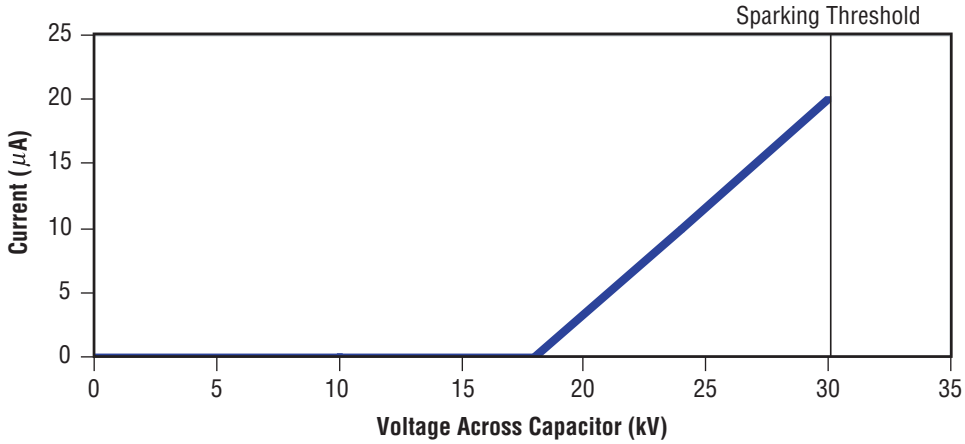

Figure 28. NACAP average current versus voltage.

By using the spin-down data, the thrust at steady state may easily be derived. The following derivation indicates the approach:

From spin-down data, the change in angular velocity with respect to time appears linear; b is intial angular velocity at t=0;

$$\omega = \frac{d\theta}{dt} = mt + b \ , \tag{9}$$

where m=slope of curve, a constant; the angular acceleration is

$$\alpha = \frac{d\omega}{dt} = \frac{d^2\theta}{dt^2} = m \ , \tag{10}$$

where ω is the angular speed and θ is the angle.

The total resistive torque, τ_R, is a combination of air resistance and bearing friction

$$\tau_R = I\alpha = I\frac{d^2\theta}{dt^2} = I\, m \ , \tag{11}$$

where I is the moment of intertia. For constant torque $\tau_{\max}$, the maximum thrust $T_{\max}$ obeys

$$\tau_R = \tau_T = T_{\max} d \ , \tag{12}$$

where d is the rotor moment arm. Hence, thrust may be calculated from the moment of inertia, the slope of the curve, and the moment arm

$$T_{\max} = \frac{I\, m}{d} \ . \tag{13}$$

This derivation provides the following thrust levels for the NACAP steady state operation:

$$T_{\text{NACAP}} = 14.54\times10^{-3} \text{ N} = 3.27\times10^{-3} \text{ lb} = 3.27 \text{ mlb} \tag{14}$$

$$\text{Thrust efficiency} = \frac{\text{mechanical output}}{\text{electrical input}} = \frac{\tau\omega}{VI}\times100\% = 3.48\% \ . \tag{15}$$

Efficiencies can probably be greatly enhanced through engineering improvements and represent a design optimization research direction for the future. The J-series thruster is one electric propulsion comparison. Operating in vacuum, it uses 5,000 W of power to produce only 45 mlb of thrust or 0.009 mlb/W. The NACAP in air produces 5.45 mlb/W. Hence, this is another indication of the promise of the NACAP as compared to other electric propulsion devices.

This analysis provides the thrust versus voltage chart shown in figure 29. Although rotation does not begin until above 20 kV, other tests have shown thrust initiation to occur as low as 8 kV.

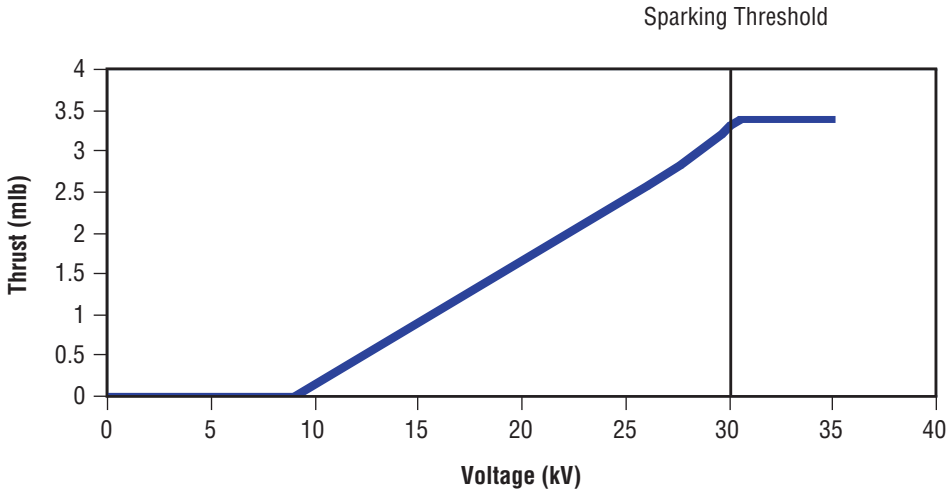

Figure 29. Thrust initiating prior to test bed rotation.

Trichel pulses associated with the NACAP were first observed at the NSSTC during operations with the NACAP. These pulses indicate the extraordinarily dynamic nature of the plasma formed in the local surroundings of the operating NACAP. The frequency of this cyclic behavior is ≈500 kHz in the radiofrequency regime (figs. 30 and 31).

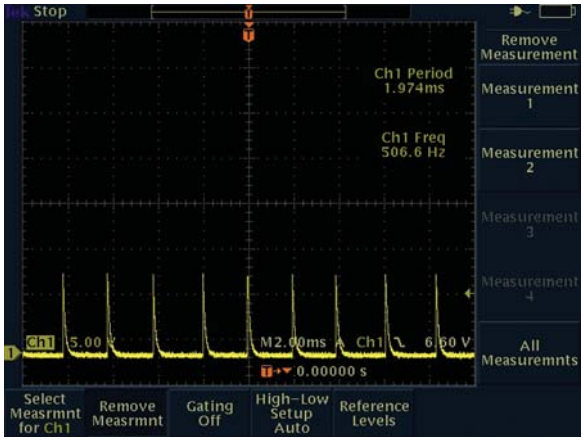

Figure 30. Cylindrical asymmetrical capacitor modules under high potential for producing thrust with Trichel pulses observed.

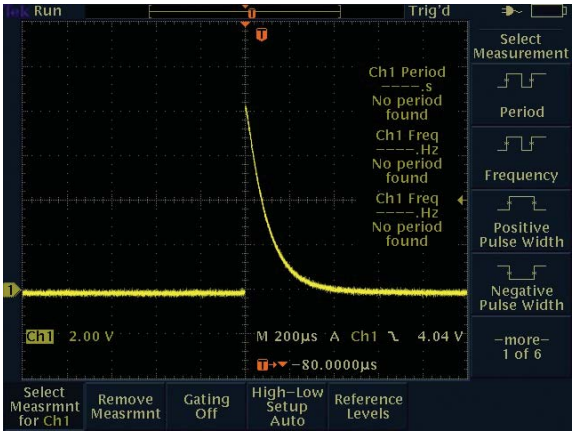

Figure 31. Cylindrical asymmetrical capacitor modules under high potential for producing thrust with Trichel pulses observed.

Table 2 illustrates the change in collision frequency and mean free path in going from 1 atm to vacuum. In vacuum, even though there is still an appreciable number of molecules present, a molecule would probably collide with the wall of the vacuum chamber before it collides with another particle. Collision frequencies are now on the order of 1/s. Clearly, loss of thrust is directly related to pressure changes.

Table 2. Collision frequency and mean free path comparison.

Pressure (torr)	Number of Molecules in Near Vicinity of NACAP	Molecular Mean Free Path (m)	Collision Frequency (collisions/s)	Temperature (K)
760	9.04×10^{21}	1.02×10^{-7}	0.46×10^{10}	300
380	TBD	2.05×10^{-7}	2.29×10^{9}	300
10^{-7}	1.19×10^{12}	0.78×10^{3}	0.6	300

6. VACUUM TESTING AND RESULTS

No performance was observed from the NACAP under soft (1 torr) or hard (10^{-7} torr) vacuum conditions. Figure 32 shows that NACAP performance rapidly falls to immeasurable levels as the pressure is reduced. In hard vacuum even with potentials above 50 kV, there was no measurable performance observed. Again, experimental runs were terminated upon reaching sparking threshold to minimize damage to the NACAP and instrumentation. For example, one precision pressure gauge was lost to electrical surges associated with sparking. Experiments included attaining normal RPM levels at 1 atm inside the vacuum chamber and then gradually bringing down the pressure while measuring changes in RPM. Measuring performance loss produced a very steep curve as pressure was reduced. Upon bringing the vacuum chamber back to 1 atm, rotation immediately began again and normal performance levels were once again attained. Figures 33 and 34 show the vacuum testing configuration.

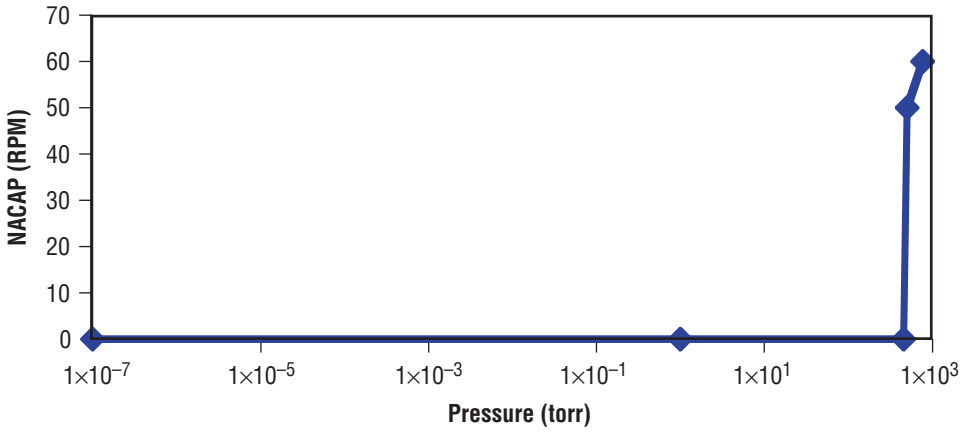

Figure 32. NACAP performance loss as pressure decreases.

Figure 33. Vacuum lab configuration.

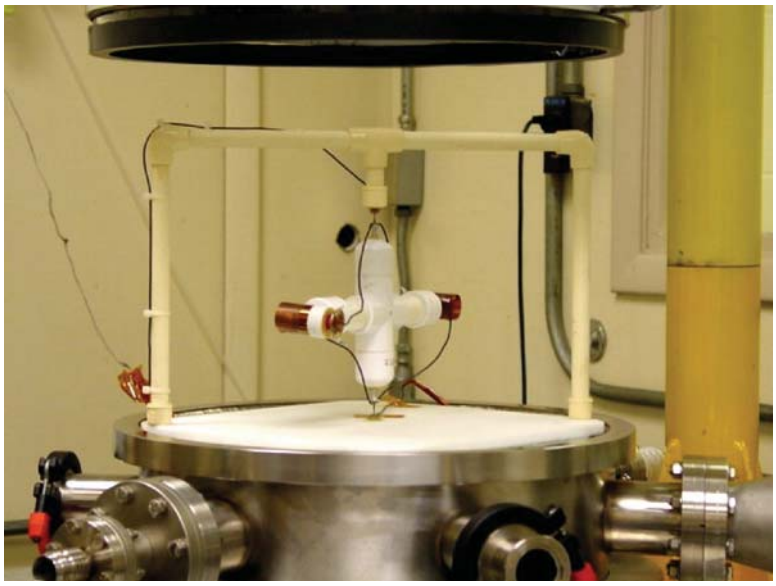

Figure 34. Closeup of two NACAPs mounted in an experimental rotational test bed for vacuum testing.

7. THEORETICAL IMPLICATIONS

A comprehensive treatment using an MHD formulation is the primary theoretical goal for future work. This treatment will include multiple loss and inefficiency mechanisms. However, a simplistic model may be used to calculate a rough upper bound. Neglecting kinetic motion of the ion and neutral gas molecules, suppose that an ionized molecule is accelerated by the electric field over a distance corresponding to the neutral mean free path until it elastically collides with a neutral. Further suppose that this ion-neutral collision stops the ion completely with respect to moving in the electric field. By conservation of momentum, the velocity of the neutral is now equal to the velocity of the ion just prior to impact; using the conservation of energy, the velocity just before impact may be estimated. For dry air at 1 atm and 80 °F, the mean free path is 1.02×10^{-7} m and the collision frequency is 0.46×10^{10} collision/s. The ion velocity just prior to impact and the neutral velocity just after impact is 695 m/s. Adding corrections for curved field lines, grazing collisions, and electrical losses gives a rough upper bound for the steady state thrust from two NACAPs of ≈100 mlb. As with the Coulomb analysis, one sees that the experimental result of a few millipounds is completely consistent with this upper bound. In other words, the observed thrust levels seem easily obtained.

The tremendous number of potential charge carriers in the immediate region around the NACAP coupled with multiple ionization mechanisms and high potential may easily provide the observed thrust levels. In other words, charged particle acceleration acting in accordance with conservation of momentum and Newton's laws (action-reaction) are sufficient to explain NACAP operation. In addition, the tremendous number of potential charge carriers in the immediate region around the NACAP offer the promise of greatly improved performance through engineering design optimization.

8. FUTURE RESEARCH AND APPLICATIONS[7]

The NACAP may be enabled for operations in space by placing a cylindrical dielectric shroud, capped at one end around the NACAP basic configuration (fig. 35). The shroud length may be varied to provide optimum operation. A gas, such as air, nitrogen, oxygen, or argon, may then be provided to the anode end of the NACAP. The NACAP then ionizes molecules and atoms in the flow and accelerates them and subsequently the neutral fluid, producing thrust. Experimentation indicates that thrust may be initiated as low as 8 kV for air. Using other gases may allow this threshold to be varied. Since thrust levels are directly proportional to voltage across the capacitor, the NACAP should also be capable of varying its thrust levels with a variable power supply. Thrust increases until reaching a sparking threshold. Operating at voltages below this threshold increases lifetime. Varying gas flow may also be a means of varying the thrust level.

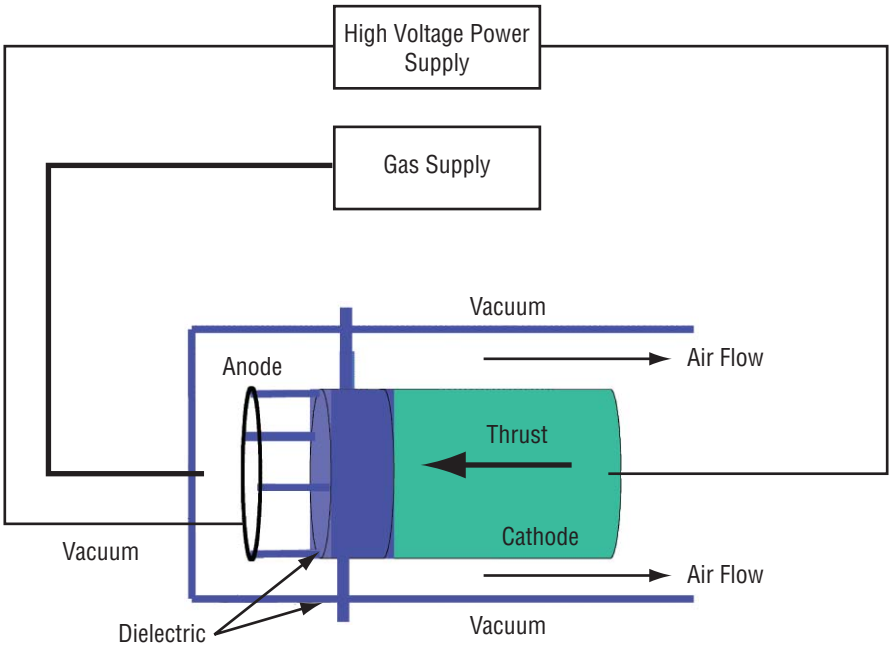

Figure 35. Shrouded NACAP for producing thrust under high voltage in space.

Shroud lengths may be varied to maximize performance (fig. 36). Cathode length is another optimization tradeoff that must be made. Increased length or diameter tends to increase thrust while also increasing weight.

Other considerations for the anode are that the conducting wire should be as fine as possible consistent with operational strength requirements. Conducting needles or screws embedded in each post allow the wire to be attached. Silver soldering or spot welding are two approaches. Any approach that preserves the electrical conductivity of the wire is acceptable. It is not necessary that the support post attached points be conductive although it seems to be a convenient design at this point (fig. 37).

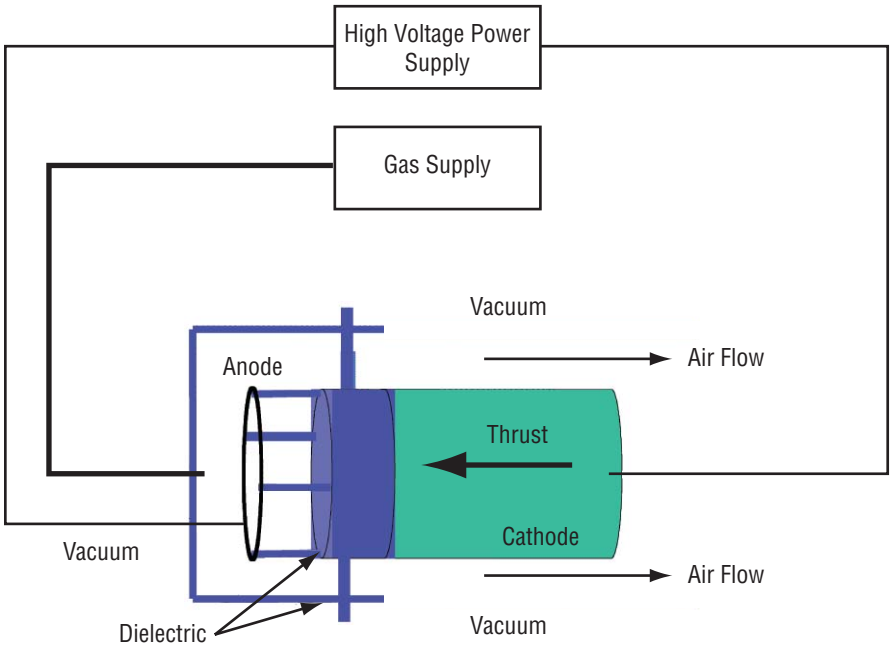

Figure 36. A shortened shrouded NACAP configuration example for producing thrust under high voltage in space.

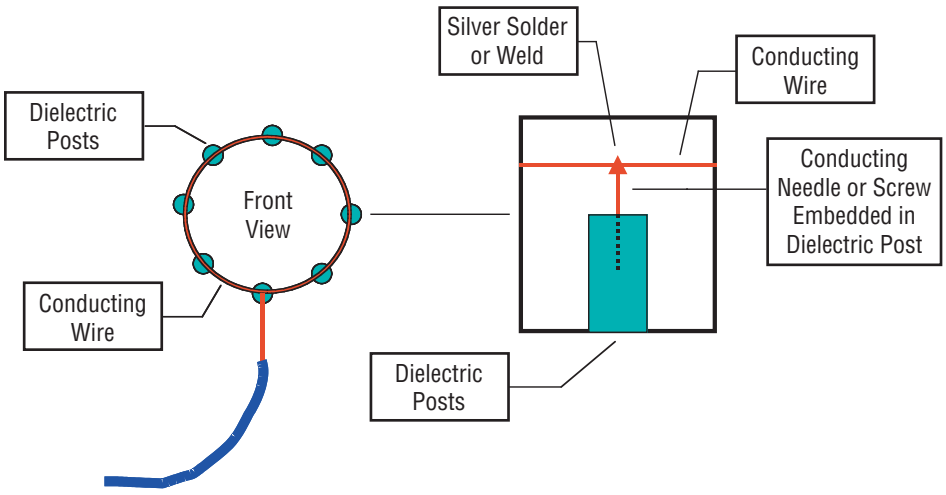

Figure 37. Additional anode configurations for NACAP I.

Fine grids may be used to increase the ionization rates of impinging neutrals (fig. 38). Another approach for using fine grids allow the entire capacitor to be built into one cylindrical surface (fig. 39). The anode may be a fine wire spiral, wire mesh, or loops of fine wire fitted and connected into a countersunk groove to improve arcing resistance. The cathode is a sheet conductor fitted and connected into a countersunk groove to improve arcing resistance. This design may be enabled for space by adding an enclosing shroud (fig. 40). Gas is provided to the anode end where it is partially ionized to provide thrust. A wire mesh anode tends to improve performance by increasing the anode corona (fig. 41).

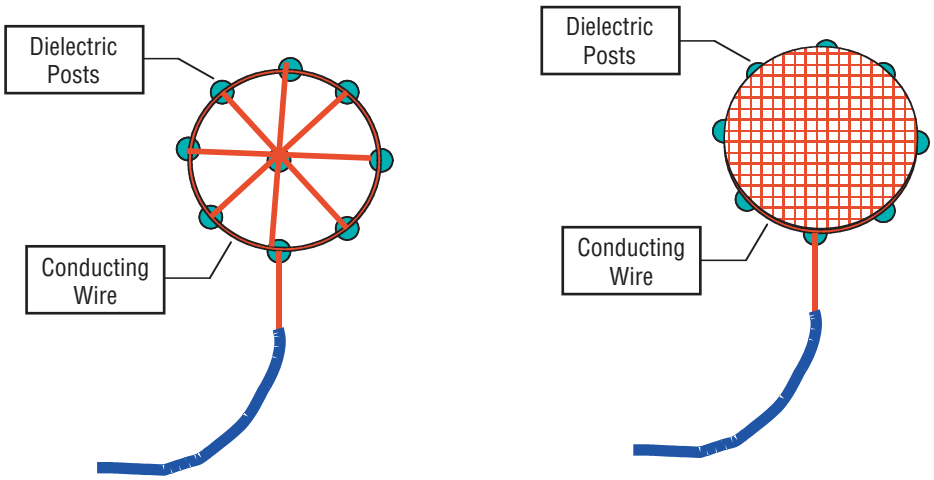

Figure 38. Additional anode configurations for NACAP II.

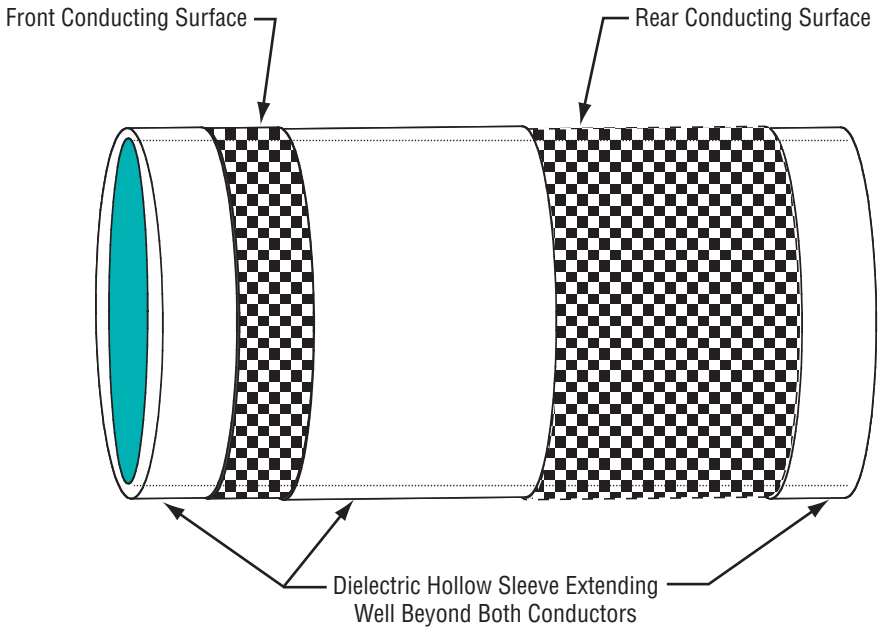

Figure 39. Basic view of performance and weight reduction design improvement for two-dimensional asymmetrical capacitor modules under high potential for producing thrust.

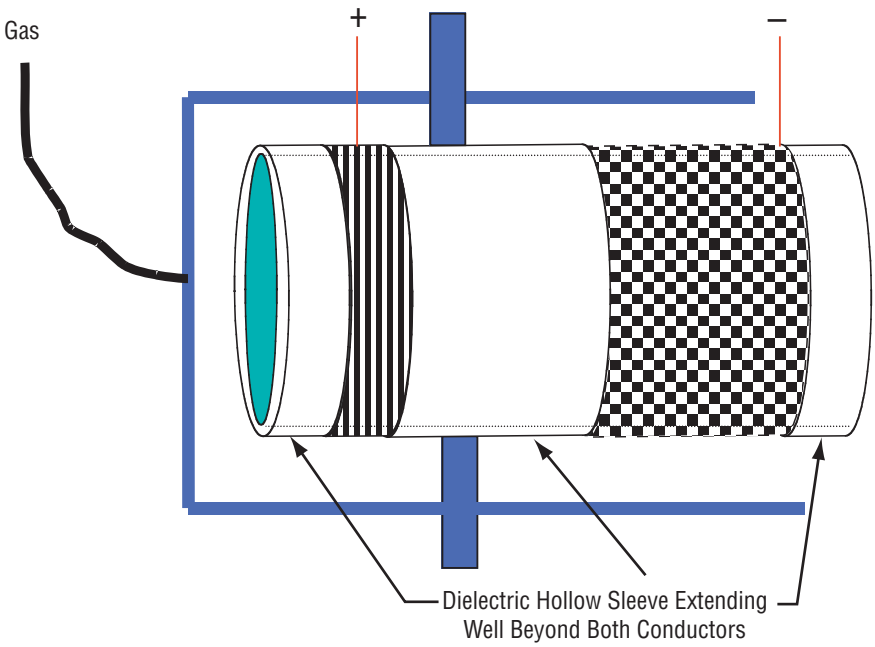

Figure 40. Another shrouded NACAP configuration for producing thrust under high voltage in space III.

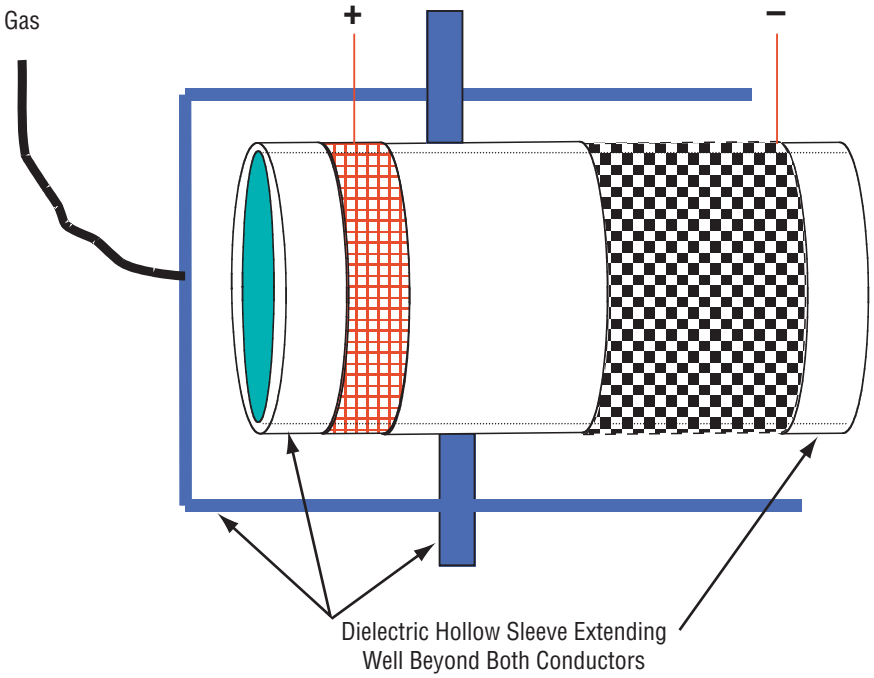

Figure 41. Another shrouded NACAP configuration for producing thrust under high voltage in space IV.

The advantage of concentrating the capacitor into a cylindrical shell is realized by placing capacitors concentrically to achieve improved performance (fig. 42). Multiple cylindrical shells may be built up as required for additional thrust. Anode wires may vary from 1 to *n*. Increasing the number of wires and shells tends to increase the thrust. Enshrouding the device and providing a gas should allow it to operate in vacuum. All devices should continue to work in air as well.

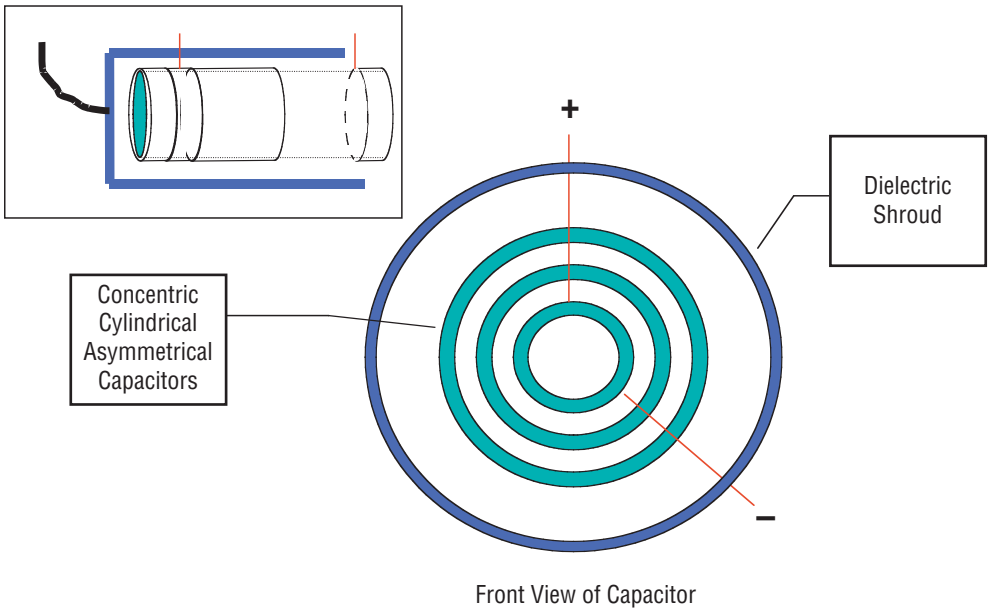

Figure 42. Shrouded NACAP nested configuration for producing thrust under high voltage in space V.

In this innovation, the NACAP effect is combined with a converging/diverging nozzle to realize a hybrid variable thrust effect in space (fig. 43). The concept should also work in air. Nozzle geometries should be optimized to achieve the greatest performance from the combined effect. The cathode is simply a sheet conductor (copper, gold, etc.) fitted and connected to lie flush with the surface of the support nozzle. Its length may be adjusted to achieve optimum performance. Its thickness may be adjusted to achieve longer lifetimes.

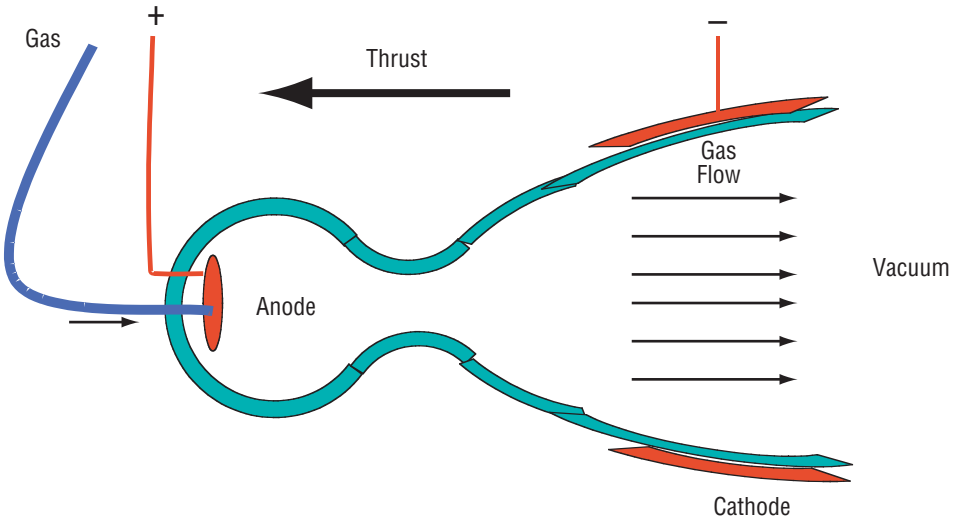

Figure 43. Enclosed anode hybrid thruster configuration of NACAP for producing thrust under high voltage in space.

The anode assembly consists of a gas supply and distribution design coupled with an anode design for producing corona. Anode wire location within a cross section of a gas supply tube may be varied to achieve optimum performance (fig. 44). Opening in annulus may be adjusted to achieve optimum performance. Again, this is one approach to increasing the anode corona (fig. 45). This approach allows the anode assembly to be simplified without loss of performance (figs. 46 and 47). Although the cylindrical configuration is optimum from an efficiency and arcing threshold point of view, other considerations from a specific application may lead to a requirement for an oval configuration or a square configuration as shown in figure 48. Either configuration should work well. Figure 49 is a side view of two low-drag concepts of another two-dimensional asymmetrical capacitor.

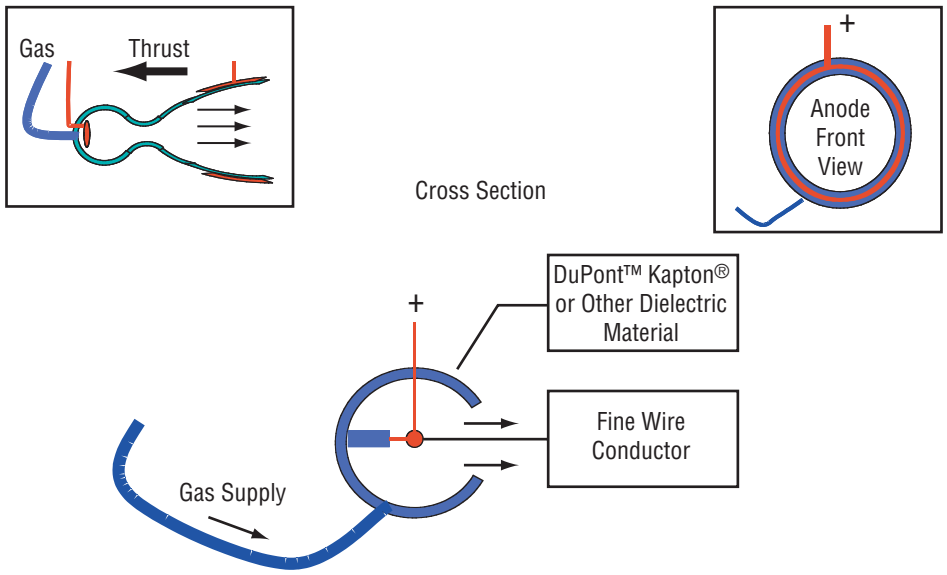

Figure 44. Enclosed anode hybrid thruster configuration of NACAP for producing thrust under high voltage in space with anode options gas tube/anode innovation I.

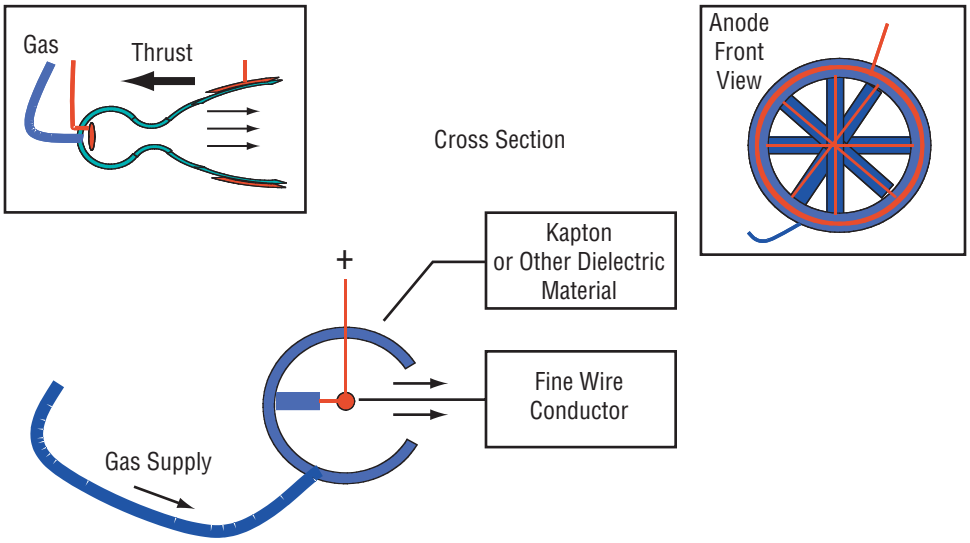

Figure 45. Enclosed anode hybrid thruster configuration of NACAP for producing thrust under high voltage in space with anode options gas tube/anode innovation II.

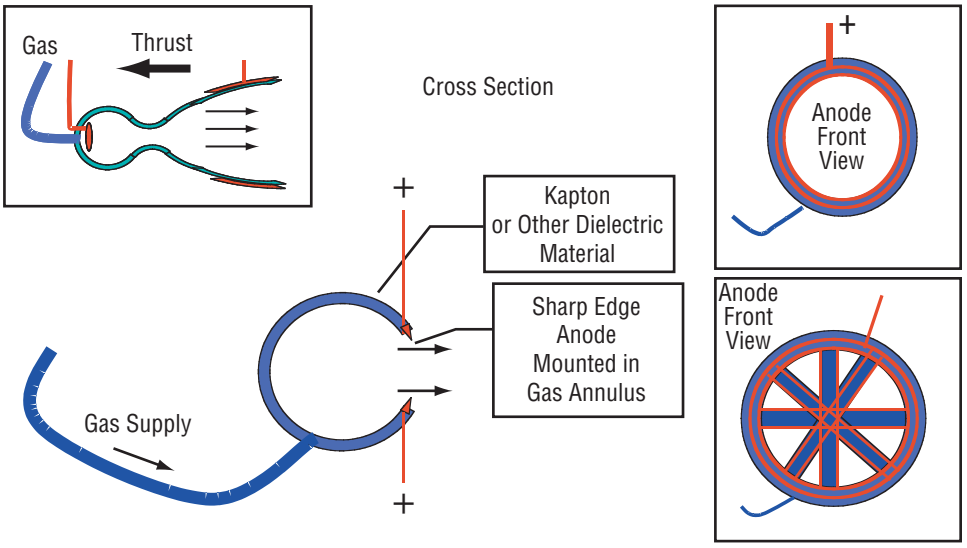

Figure 46. Enclosed anode hybrid thruster configuration of cylindrical asymmetrical capacitor for producing thrust under high voltage in space III.

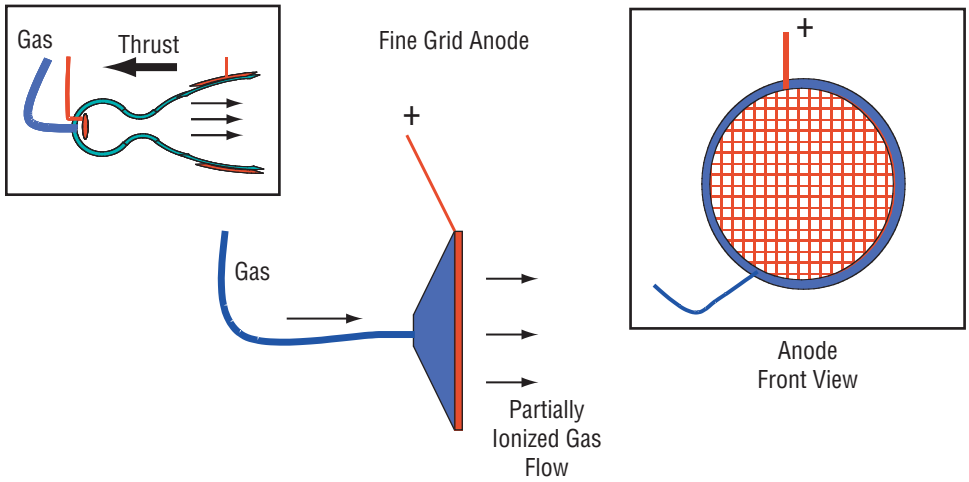

Figure 47. Enclosed anode hybrid thruster configuration of cylindrical asymmetrical capacitor for producing thrust under high voltage in space with anode options gas tube/anode innovation IV.

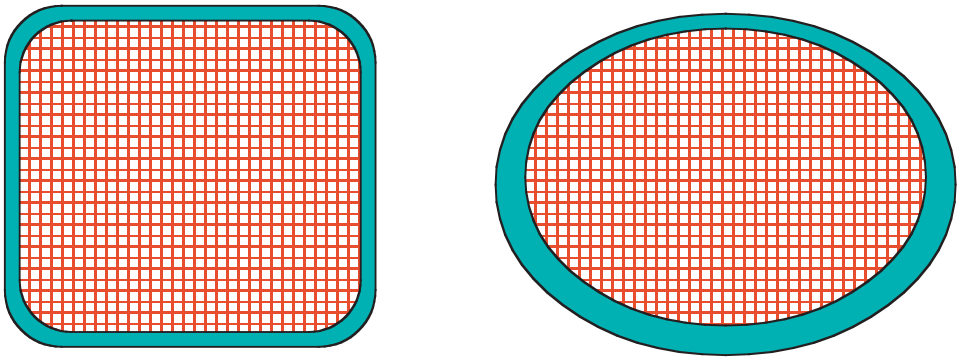

A square shape or an elliptical shape may also be employed as required by the particular application.

Figure 48. Front view of two-dimensional NACAP configurations for producing thrust under high voltage in space.

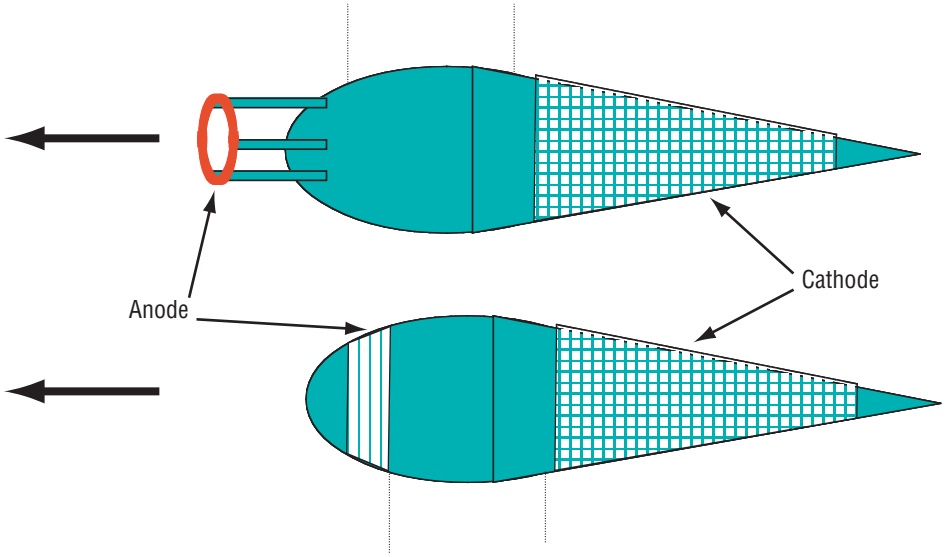

Figure 49. Side view of two low-drag concepts of a two-dimensional asymmetrical capacitor for producing thrust under high voltage in space.

Thruster performance may be more easily optimized during operation by providing the means to continuously vary anode/cathode separation, voltage, and current depending upon environmental conditions such as humidity, pressure, and sparking likelihood. In this design, this may be accomplished by having a computer controller sensing separation, current, and voltage and adjusting the anode appropriately to optimize thrust while avoiding sparking (figs. 50 and 51).

Depending upon the availability of funding, future NACAP research should be focused on engineering design optimization for aerospace applications; experimental efforts shall be bolstered by a theoretical MHD analysis. This research will attempt to realize the promise for improved performance of the technology while meeting general aerospace requirements including structural robustness and safety. In air, the NACAP may have application for improving helicopter rotor performance and serving as the primary propulsion system for high lift and long loiter platforms, such as powered gliders and dirigibles. The NACAP may prove to be a convenient propulsion system for use with beamed power applications. In space with design enhancements, the NACAP may have applicability as an attitude control system or in other in-space electric propulsion applications. Application will depend upon NACAP performance as compared to existing technologies. In addition, the research should be useful for educational outreach.

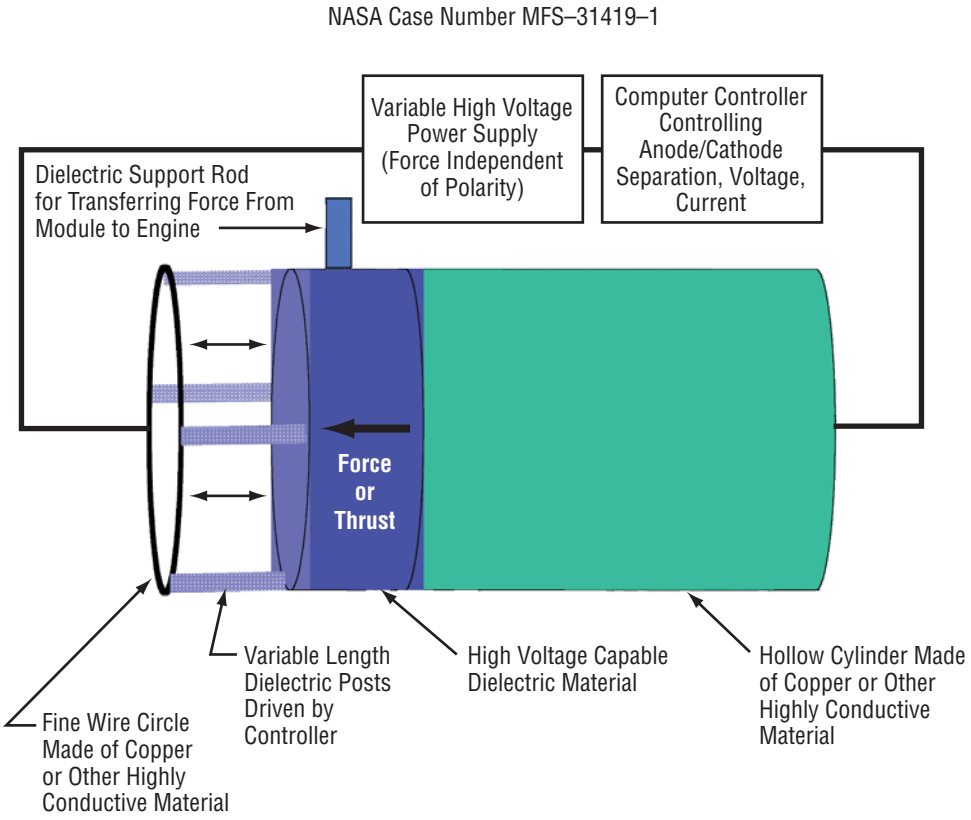

Figure 50. Illustration showing that adding a current/voltage controller may significantly enhance operational performance.

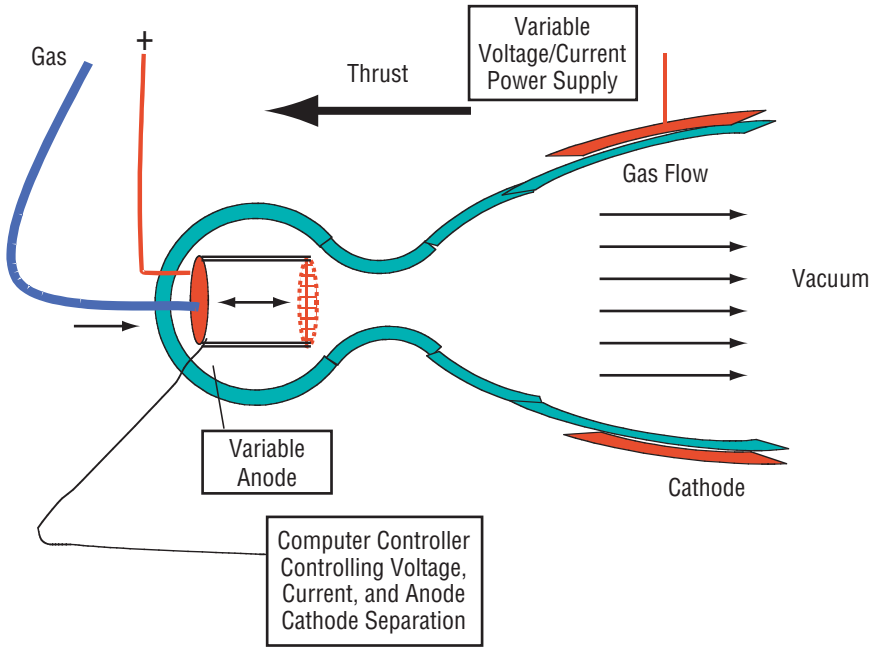

Figure 51. Enclosed anode hybrid thruster configuration with variable anode/cathode separation.

9. SUMMARY AND CONCLUSIONS

The NACAP was derived/synthesized solely and entirely from extensive open source, public domain databases. Hundreds of hours of observations all indicate that the NACAP obeys the laws of physics as currently understood including MHD equations, conservation of momentum, Coulomb's law, and Newton's laws of motion. Given the tremendous numbers of charge carriers available in the near vicinity of the NACAP and electromagnetic forces acting at the speed of light, accelerated particles are easily sufficient to explain observed levels of performance. No NACAP performance was observed in vacuum, implying reduced thrust levels as the numbers of potential charge carriers were reduced. However, what remains is a structurally robust propulsion device that produces thrust in air using no onboard fuel and no moving parts. It should also be noted that the NACAP configuration lends itself to maximum safety operations. Depending upon the availability of funding and the level of success achieved in NACAP optimization, the technology may or may not find a niche as an aerospace application. Only continued optimization research shall provide an answer for this question.

APPENDIX A—OUTREACH EFFORTS

As part of outreach efforts, the authors supported a high school student, Evan Frank, with his science fair project (fig. 52). His father wrote in 2003:

"It is with sincere thanks and pleasure that I inform you that my son's project on Dr. Campbell's patent has garnered:

- Top physics project, Louisville region
- Top physics and engineering project award from the University of Louisville Speed Scientific School
- Air Force top project award qualifying him to compete at a National USAF competition, celebrating the 100th anniversary of flight at Wright Patterson Air Force Base in Dayton later this spring
- Top Navy technical award
- Evan was selected for one of two individual slots from the region to the International Science Fair this year in Cincinnati

Guys, this is huge, and I just wanted to express my gratitude for your willingness to spend some time kindling the spark of creativity and inventiveness! Best Personal Regards—Jeff."

Evan went on to win a $20,000 scholarship at the international science fair in 2003. He is having great success again this year with this technology having won several awards at his regional science fair and, for the second consecutive year in a row, a chance to compete in the 2004 science fair. At the international science fair, he won second place in physics and cash awards totaling several hundred dollars. He plans to join the Alabama A&M Starflight Team this summer at Johnson Space Center to fly the NACAP in a variable-g environment as a student experiment onboard the NASA KL135 aircraft.

Figure 52. Evan Frank's award-winning science fair project.

APPENDIX B—PRINCIPAL INVESTIGATOR BACKGROUND

The NACAP principal investigator is Dr. Jonathan W. Campbell. He is currently assigned to the Advanced Projects Office, Flight Projects Directorate, NASA MSFC and has over 25 years experience in the area of advanced aerospace technologies. He has published over 75 papers and has through his innovation initiatives been successful in winning several patents for NASA and the taxpayer.

Dr. Campbell's experience with capacitors goes back to his grammar school science fair competition where he built a basic capacitor from aluminum foil, waxed paper, and cardboard as part of a crystal radio project. He built all components of the radio with the exception of the crystal and integrated them. The radio worked and he won the competition.

Awarded a bachelor's degree in aerospace engineering, Dr. Campbell was exposed to many propulsion ideas both conventional and conceptual. This was his first introduction to electric propulsion systems and to Townsend Brown's work.

As a master's candidate at Auburn in experimental plasma physics, he worked with high voltages to create transient helium plasmas for characterization. Large capacitor banks were needed for transient discharges and arcing was a recurrent problem. He designed and redesigned capacitor modification after modification to try and manage arcing problems. Once, a visitor was present when a spurious arcing event occurred across the bank. He commented that there was lightning running around the lab. NACAPs operate at similar voltages and managing sparking is a major undertaking in the optimization of these devices. Dr. Campbell's master's thesis was entitled "Measurements Taken on a Transient Helium Plasma Using a Magnetic Probe And Other Diagnostic Techniques."

This experience would later be useful in working with the J-series electric propulsion technologies that he would encounter his first year at NASA. These thrusters ionized liquid mercury and then accelerated the charged ions using electric fields. The charged ions leaving the system resulted in thrust. This experience with electric propulsion would create a lasting research interest.

Later in his career as part of his Ph.D. dissertation research he worked extensively with solar flare plasma kinetic and dynamic theory. MHD theory, tailored with the appropriate boundary conditions and assumptions, may be used to describe the complex behavior of the plasma, particle, and field interactions in a flaring loop the size of Earth in the Sun's atmosphere. Similarly, a correctly formulated MHD description may also be used to describe on a much smaller scale the NACAP's complex physics.

REFERENCES

1. Talley, R.L.: "Twenty First Century Propulsion Concept," *PLTR–91–3009*, Veritay Technology, Inc., East Amherst, NY, Final Report for the period February 1989 to July 1990, Contract FO4611–89–C–0023, Phillips Laboratory, Air Force Systems Command, Edwards Air Force Base, CA, May 1991.

2. Advanced Propulsion Technology Group, Jet Propulsion Laboratory, Caltech, Pasadena, CA, http://www.islandone.org/APC/index.html, http://www.islandone.org/APC/Electric/00.html.

3. Brown, T.T.: "A Method of and an Apparatus or Machine for Producing Force," British Patent No. 300,311, November 15, 1928.

4. Brown, T.T.: "Electrokinetic Apparatus," U.S. Patent No. 2,949,550, August 16, 1960.

5. Campbell, J.W.: "Apparatus and Method for Generating Thrust Using a Two Dimensional, Asymmetrical Capacitor Module," U.S. Patent No. 6,317,310 B1, November 13, 2001.

6. Campbell, J.W.: "Apparatus for Generating Thrust Using a Two Dimensional, Asymmetrical Capacitor Module," U.S. Patent No. 6,411,493 B2, June 25, 2002.

7. Campbell, J.W.: "Cylindrical Asymmetrical Capacitor Devices for Space Applications," NACAP patent, NASA Case No. MFS–31887–1, U.S. Patent No. TBD.

REPORT DOCUMENTATION PAGE

Form Approved
OMB No. 0704-0188

1. AGENCY USE ONLY *(Leave Blank)*	2. REPORT DATE	3. REPORT TYPE AND DATES COVERED
	June 2004	Technical Memorandum

4. TITLE AND SUBTITLE

NASA Marshall Space Flight Center Barrel-Shaped Asymmetrical Capacitor

5. FUNDING NUMBERS

6. AUTHORS

J.W. Campbell, M.R. Carruth, D.L. Edwards, A. Finchum, G. Maxwell, S. Nabors, L. Smalley,* D. Huston,** D. Ila,** R. Zimmerman,** C. Muntele,** and I. Muntele**

7. PERFORMING ORGANIZATION NAMES(S) AND ADDRESS(ES)

George C. Marshall Space Flight Center
Marshall Space Flight Center, AL 35812

8. PERFORMING ORGANIZATION REPORT NUMBER

M–1115

9. SPONSORING/MONITORING AGENCY NAME(S) AND ADDRESS(ES)

National Aeronautics and Space Administration
Washington, DC 20546–0001

10. SPONSORING/MONITORING AGENCY REPO NUMBER

NASA/TM—2004–213283

11. SUPPLEMENTARY NOTES

Prepared by the Advanced Projects Office, Flight Projects Directorate
*The University of Alabama in Huntsville **Alabama A&M University

12a. DISTRIBUTION/AVAILABILITY STATEMENT

Unclassified-Unlimited
Subject Category 12
Available: NASA CASI 301–621–0390

12b. DISTRIBUTION CODE

13. ABSTRACT *(Maximum 200 words)*

The NASA Barrel-Shaped Asymmetrical Capacitor (NACAP) has been extensively tested at NASA Marshall Space Flight Center and the National Space Science and Technology Center. Trichel pulse emission was first discovered here. The NACAP is a magnetohydrodynamic device for electric propulsion. In air it requires no onboard propellant nor any moving parts. No performance was observed in hard vacuum. The next step shall be optimizing the technology for future applications.

14. SUBJECT TERMS

asymmetrical capacitor, electric propulsion, magnetohydrodynamics, ion acceleration, ion wind

15. NUMBER OF PAGES

64

16. PRICE CODE

17. SECURITY CLASSIFICATION OF REPORT	18. SECURITY CLASSIFICATION OF THIS PAGE	19. SECURITY CLASSIFICATION OF ABSTRACT	20. LIMITATION OF ABSTRACT
Unclassified	Unclassified	Unclassified	Unlimited